1 Ammonium-adduct chemical ionization to investigate
2 anthropogenic oxygenated gas-phase organic compounds in
3 urban air

5 Peeyush Khare[1,¶], Jordan E. Krechmer[2], Jo Ellen Machesky[1], Tori Hass-Mitchell[1], Cong Cao[3],
6 Junqi Wang[1], Francesca Majluf[2,**], Felipe Lopez-Hilfiker[4], Sonja Malek[1], Will Wang[1], Karl
7 Seltzer[5], Havala O.T. Pye[6], Roisin Commane[7], Brian C. McDonald[8], Ricardo Toledo-Crow[9], John
8 E. Mak[3], Drew R. Gentner[1,10]

10 [1]Department of Chemical and Environmental Engineering, Yale University, New Haven CT-06511 USA
11 [2]Aerodyne Research Inc. Billerica MA- 02181 USA
12 [3]School of Marine and Atmospheric Science, Stony Brook University, Stony Brook NY-11794 USA
13 [4]Tofwerk AG, CH-3600 Thun, Switzerland
14 [5]Office of Air and Radiation, Environmental Protection Agency, Research Triangle Park, NC-27711 USA
15 [6]Office of Research and Development, Environmental Protection Agency, Research Triangle Park, NC-
16 27711 USA
17 [7]Department of Earth and Environmental Sciences, Lamont-Doherty Earth Observatory, Columbia
18 University, New York, NY-10027 USA
19 [8]Chemical Sciences Laboratory, National Oceanic and Atmospheric Administration, Boulder CO- USA
20 [9]Advanced Science Research Center, City University of New York, New York, NY-10031 USA
21 [10]School of the Environment, Yale University, New Haven CT-06511 USA
22 [¶]now at: Laboratory of Atmospheric Chemistry, Paul Scherrer Institute, Villigen AG-5232 Switzerland
23 ** now at: Franklin W. Olin College of Engineering (fmajluf@olin.edu, (781) 292-2300).

25 Corresponding authors: Jordan E. Krechmer (krechmer@aerodyne.com) and Drew R. Gentner
26 (drew.gentner@yale.edu)

28 Abstract

29 Volatile chemical products (VCPs) and other non-combustion-related sources have
30 become important for urban air quality, and bottom-up calculations report emissions of a
31 variety of functionalized compounds that remain understudied and uncertain in emissions
32 estimates. Using a new instrumental configuration, we present online measurements of
33 oxygenated VCPs in a U.S. megacity over a 10-day wintertime sampling period, when
34 biogenic sources and photochemistry were less active. Measurements were conducted at a
35 rooftop observatory in upper Manhattan, New York City, USA using a Vocus chemical
36 ionization time-of-flight mass spectrometer with ammonium (NH_4^+) as the reagent ion
37 operating at 1 Hz. The range of observations spanned volatile, intermediate-volatility, and
38 semi-volatile organic compounds with targeted analyses of ~150 ions whose likely
39 assignments included a range of functionalized compound classes such as glycols, glycol
40 ethers, acetates, acids, alcohols, acrylates, esters, ethanolamines, and ketones that are
41 found in various consumer, commercial, and industrial products. Their concentrations
42 varied as a function of wind direction with enhancements over the highly-populated areas
43 of the Bronx, Manhattan, and parts of New Jersey, and included abundant concentrations

44 of acetates, acrylates, ethylene glycol, and other commonly-used oxygenated compounds.
45 The results provide top-down constraints on wintertime emissions of these
46 oxygenated/functionalized compounds with ratios to common anthropogenic marker
47 compounds and compares their relative abundances to two regionally-resolved emissions
48 inventories used in urban air quality models.

49

50 **Keywords:** Volatile chemical products, non-combustion-related emissions, personal care
51 products, solvents, glycol ethers, VOCs, IVOCs, SVOCs, urban air quality, New York
52 City, LISTOS, AEROMMA

53

54 **1. Introduction**

55 Non-combustion-related sources are increasingly important contributors of anthropogenic
56 emissions in developed regions and megacities with implications for tropospheric ozone
57 and secondary organic aerosols (SOA) (Coggon et al., 2021; Khare and Gentner, 2018;
58 Mcdonald et al., 2018; Pennington et al., 2021; Shah et al., 2020). These sources include
59 volatile chemical products (VCPs), asphalt, and other products/materials that emit
60 volatile-, intermediate- and semi-volatile organic compounds (VOCs, IVOCs, SVOCs),
61 which contribute to the atmospheric burden of reactive organic carbon (ROC) (Heald and
62 Kroll, 2020). Emissions occur over timescales ranging from minutes to several days and
63 up to years in some cases (Khare and Gentner, 2018). Compounds from VCPs are diverse
64 in terms of chemical composition and depend on application methods and uses of
65 different products and materials. Examples of compound classes found in consumer and
66 commercial products include hydrocarbons, acetates, alcohols, glycols, glycol ethers,
67 fatty acid methyl esters, aldehydes, siloxanes, ethanolamines, phthalates and acids (Bi et
68 al., 2015; Even et al., 2019, 2020; Khare and Gentner, 2018; Mcdonald et al., 2018).

69

70 A subset of compounds from these classes have been investigated in indoor environments
71 for sources like building components (e.g. paints), household products (e.g. cleaners,
72 insecticides, fragrances), and for some from polymer-based items such as textiles and
73 toys (Bi et al., 2015; Even et al., 2020; Harb et al., 2020; Liang et al., 2015; Noguchi and
74 Yamasaki, 2020; Shi et al., 2018; Singer et al., 2006). Emissions are often dependent on
75 volatilization and thus can exhibit dependence on temperature (Khare et al., 2020).
76 However, other environmental factors such as relative humidity can sustain or enhance
77 indoor air concentrations of a wide range of compounds including alcohols, glycols and
78 glycol ethers for months after application of paints (Choi et al., 2010b; Markowicz and
79 Larsson, 2015). Similarly, mono-ethanolamines from degreasers and oxygenated third-

80 hand cigarette smoke compounds have also been shown to off-gas and persist in indoor
81 air for days or more after application or use (Schwarz et al., 2017; Sheu et al., 2020).

82

83 Non-combustion-related emissions of ROC can present health risks through direct
84 exposure in both indoor and outdoor environments and via SOA and ozone production
85 (Bornehag et al., 2005; Choi et al., 2010a; Destaillats et al., 2006; Masuck et al., 2011;
86 Pye et al., 2021; Qin et al., 2020; Wensing et al., 2005). These health impacts will be
87 modulated by the rate at which indoor emissions of ROC are transferred outdoors (Sheu
88 et al., 2021), but indoor sinks are uncertain and have often been neglected in emissions
89 inventory development for VCPs until recently (McDonald et al., 2018; Seltzer et al.,
90 2021b). Information on indoor and outdoor concentrations of many ROC compounds is
91 limited due to the historical focus on more volatile hydrocarbons and small oxygenated
92 compounds (e.g. methanol, isopropanol, acetone) and shorter timescales of solvent
93 evaporation (e.g. <1 day). In comparison, emissions of intermediate- and semi-volatile
94 compounds (I/SVOCs; including higher molecular weight oxygenates) and some
95 chemical functionalities (e.g. glycol ethers) are poorly constrained, owing to
96 instrumentation challenges and/or long emission timescales (Khare and Gentner, 2018).

97

98 Single-ring aromatic VOCs (e.g. benzene, toluene, ethylbenzene, xylenes) have
99 historically been well-known contributors to urban ozone and SOA production (Henze et
100 al., 2008; Venecek et al., 2018). On this basis, regulatory policies drove a shift towards
101 oxygenates to replace these aromatics and other unsaturated hydrocarbons as solvents
102 (Council of the European Union, 1999), which has influenced the ambient composition
103 of oxygenated volatile organic compounds (OVOCs) (Venecek et al., 2018). Recent top-
104 down measurements have revealed large upward fluxes of OVOCs in urban environments
105 that double the previous urban anthropogenic emission estimates (Karl et al., 2018).
106 Other studies have found substantial VCP emissions (e.g. Decamethylcyclopentasiloxane
107 or D5) to outdoor environments in several large cities such as Boulder, CO; New York,
108 NY; Los Angeles, CA and Toronto, Canada (Coggon et al., 2018, 2021; Gkatzelis et al.,
109 2021b, 2021a; Khare and Gentner, 2018; Mcdonald et al., 2018; McLachlan et al., 2010).
110 Offline laboratory experiments with select VCP-related precursors have also shown
111 significant SOA yields from oxygenated aromatic precursors (Charan et al., 2020; Humes
112 et al., 2022). Furthermore, bottom-up estimates suggest that 75-90% of the non-
113 combustion emissions are constituted by functionalized species while only the remaining
114 10-25% are hydrocarbons (Khare and Gentner, 2018; Mcdonald et al., 2018).

115

116 To improve observational constraints on the abundances of widely-used oxygenated
117 VCPs that are expected to influence urban air quality, but are uncertain in emissions
118 inventories, we employed a Vocus chemical ionization time-of-flight mass spectrometer
119 (Vocus CI-ToF) using ammonium (NH_4^+) as a chemical reagent ion to increase
120 sensitivity to compound types that have traditionally provided measurement challenges.
121 Specifically, we: (a) evaluated the performance of the CI-ToF for a diverse array of
122 oxygenated VCPs and compare ambient observations between NH_4^+ and H_3O^+ reagent
123 ions; (b) examined ambient abundances of a subset of oxygenated gas-phase organics
124 related to VCP emissions and their dynamic atmospheric concentrations in New York
125 City (NYC) over a 10-day winter period with reduced biogenic emissions and secondary
126 OVOC production; (c) determined their ambient concentration ratios and covariances
127 with major tracer compounds; and (d) compared ambient observations against two
128 regionally-resolved emissions inventories to provide top-down constraints on the relative
129 emissions of major oxygenated VCPs that influence urban air quality. The findings of this
130 work highlight the diversity of functionalized organic species emitted from VCPs with
131 comparisons against inventories that inform our understanding of VCP composition and
132 emission pathways, and thus improve urban air quality models and policy.

133

134 **2. Materials and methods**

135 The sampling site was located at the Rooftop Observatory at the Advanced Science
136 Research Center of the City University of New York (CUNY ASRC, 85 St. Nicholas
137 Terrace) in Upper Manhattan (Figures S1-2), which is the location of the Manhattan
138 ground site for the upcoming AEROMMA research campaign (Warneke et al., n.d.). The
139 ASRC is built on top of a hill 30 m above the mean sea level whose surface is naturally
140 elevated above the surrounding landscape. The observatory is 86 m above the mean sea
141 level and the inlet was at 89 m with minimally obstructed views to the northwest and east
142 towards the Bronx and Harlem, as well as to the south along the island of Manhattan.
143
144
145 Gas-phase VOCs and I/SVOCs were measured using a Vocus CI-ToF with a NH_4^+
146 reagent ion source (Krechmer et al., 2018), which had a higher sensitivity than most
147 previous state-of-the-art chemical ionization-ToF instruments, a mass resolving power of
148 ~10,000 m/Δm, and was quantitatively independent of ambient humidity changes (Figure
149 1a). The Vocus CI-TOF sampled at a frequency of 1 Hz continuously throughout the 10-
150 day period from 21st to 31st January 2020. NH_4^+ ionization coupled with high frequency
151 online mass spectrometry enables measurements of functionalized compounds emitted
152 from diverse, distributed sources in around New York City. Ammonium has a long
153 history of use as a positive-ion reagent gas in chemical ionization mass spectrometry, but
154 has only recently been applied to the study of atmospheric chemistry with time-of-flight

155 mass spectrometers (Canaval et al., 2019; Westmore and Alauddin, 1986; Zaytsev et al.,
156 2019b, 2019a). The NH_4^+ reagent ion forms clusters effectively with polarizable
157 molecules, providing mostly softly ionized NH_4^+-molecule adducts, though some
158 protonation, charge transfer, and fragmentation can occur as alternate ionization
159 pathways (Canaval et al., 2019). It has previously been applied in laboratory studies in
160 different configurations than the instrument described here (Canaval et al., 2019; Zaytsev
161 et al., 2019b), and to our knowledge this is the first published atmospheric field
162 measurement with NH_4^+ionization.
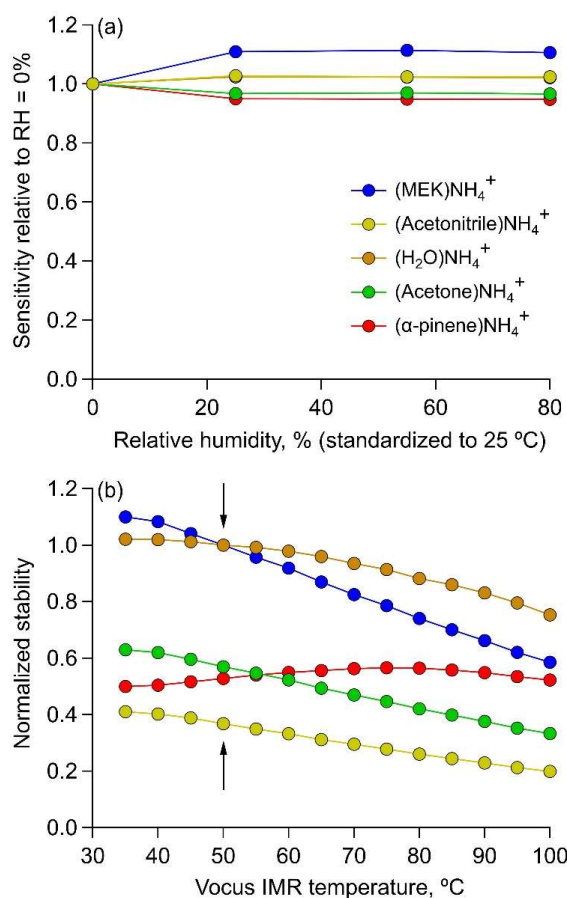
163
164
165 **Figure 1: Vocus CI-ToF performance with low-pressure NH_4^+ ionization as a**
166 **function of atmospheric conditions and instrument parameters. (a) Minimal effects**
167 **of relative humidity (RH) on Vocus CI-ToF quantification for several major**
168 **compounds using the NH_4^+ Vocus CI-ToF (b) Ion-adduct stability as a function of**
169 **temperature in the focusing Ion Molecule Reaction (fIMR) region, with ambient**
170 **measurements made at 50 °C in this study.**

171
172
173 NH$_4^+$ selectively ionizes functionalized species including ones that have generally been
174 difficult to measure using proton-transfer reaction ionization due to excess fragmentation
175 (e.g. glycols) or low proton affinities (Karl et al., 2018). However, it excludes non-polar
176 hydrocarbons and is not intended to examine emissions from hydrocarbon-dominated
177 non-combustion sources (e.g. mineral spirits, petroleum distillates).
178
179
180 To produce NH$_4^+$ reagent ions in the Vocus focusing ion molecule reactor (fIMR), 20
181 sccm of water (H$_2$O) vapor and 1 sccm of vapor from a 1% ammonium hydroxide in H$_2$O
182 solution were injected into the discharge ion source. In addition to forming (NH$_4^+$) H$_2$O
183 as the primary reagent ion, the relatively large amount of water buffers the source against
184 any changes in relative humidity, removing any quantitative humidity dependence and
185 the need for humidity-dependent calibrations. This lack of RH-dependence is shown in
186 Figure 1. The Vocus axial voltage was maintained at a potential difference of 425 V and
187 the reactor was maintained at a pressure of 3.0 mbar and temperature of 50 °C (to
188 maximize thermal stability as shown in Figure 1b), which corresponds to an E/N value of
189 70 Td. Additional characterization tests, including scans of the voltage differentials, are
190 shown in Figure S3 and were used to inform our choice of instrument settings for the
191 ambient measurements.
192
193
194 The instrument inlet was set up at the southeast corner of the observatory. 100 sccm of air
195 was subsampled into the Vocus CI-ToF from a Fluorinated Ethylene Propylene (FEP)
196 Teflon inlet 5 m long and with a 12.7 mm outer diameter that had a flowrate of 20 liters
197 min^{-1} resulting in a residence time of ~ 1 s. Importantly for measurements of semi-volatile
198 VCPs, no particulate filter was used on the inlet to enhance transmission of semi- and
199 low-volatility gases (Krechmer et al., 2016; Pagonis et al., 2017).
200
201
202 The instrument background was measured every 15 minutes for 1 minute by injecting
203 purified air generated by a Pt/Pd catalyst heated to 400 °C. Every 4 hours, diluted
204 contents from a 14-component calibration cylinder (Apel-Riemer Environmental) were
205 injected for 1 minute to measure and track instrument response over time (Table S1). To
206 quantify CI-ToF signals for additional VCPs of interest, after the campaign we injected
207 prepared quantitative standards of specific water-soluble VCPs that were observed in
208 field measurements into the instrument from a Liquid Calibration System (LCS;
209 TOFWERK AG) and measured the instrument response to create multi-point calibration
210 curves. The LCS standards were then normalized using the cylinder calibrations during

211   and after the campaign with the same tank. Although the CI-ToF used the same settings
212   for calibrations as in the campaigns, this normalization accounted for differences in the
213   instrument performance during and after the campaign. A table of the standard
214   compounds along with their instrument responses can be found in Table S2.
215
216
217   Data were processed using Tofware version 3.2.3 (Aerodyne Research, Inc.) in the Igor
218   Pro programming environment (Wavemetrics, Inc.). Compounds of interest were detected
219   as NH_4^+ adducts within 2 ppm mass accuracy, but for clarity we refer to detected signals
220   after subtracting the ammonium adduct (e.g. C_3H_6O instead of $(NH_4) C_3H_6O^+$) in the
221   Results and Discussion section below. For this focused analysis of urban emissions, data
222   filtering was also performed on a subset of compounds to remove the influence of
223   biomass burning events which resulted in elevated benzene to toluene ratios during
224   inflow of air from the less densely populated western direction. These additional
225   contributions from biomass burning-related emissions would not be included in the
226   inventoried emissions and would bias calculations of urban emission ratios in this study.
227   Hourly periods with large contributions from biomass burning were filtered for affected
228   compounds using a benzene-to-toluene ratio >2. Thus, elevated concentrations of
229   oxygenated compounds coincided with inflow from the more densely populated areas of
230   the city.
231
232
233   In addition to online measurements, a subset of adsorbent tube samples were also
234   collected during Winter 2020 for offline analysis using gas chromatography electron
235   ionization mass spectrometry (GC EI-MS) (Sheu et al., 2018) and were used here to
236   confirm the identifications of oxygenated VCPs measured as molecular formulas by the
237   online CI-TOF. Additional measurements of meteorological parameters (e.g. wind
238   speed/direction) (ATMOS 41 weather station) and carbon monoxide (Picarro G2401m)
239   were also collected at the sampling site. A co-located high-resolution proton-transfer-
240   reaction time-of-flight mass spectrometer (Ionicon Analytik PTR-ToF 8000) from Stony
241   Brook University also made coincident long-term measurements, some of which were
242   used to validate the performance of the CI-TOF with NH_4^+ ionization.
243
244
245   Annual emissions from VCPs in NYC counties were estimated using VCPy.v2.0 (Seltzer
246   et al., 2021, 2022). Additional NYC-resolved comparisons are made with the FIVE-VCP
247   emissions inventory developed at the U.S. National Oceanic and Atmospheric
248   Administration using methods described by McDonald et al. (Mcdonald et al., 2018) and
249   updated for New York City in Coggon et al. (Coggon et al., 2021). A major update in the
250   latter study was updating the VCP speciation profiles to the most recent surveys of
251   consumer products, fragrances and architectural coatings. In VCPy, the magnitude and

252   speciation of organic emissions are directly related to the mass of chemical products
253   used, the composition of these products, the physiochemical properties of the chemical
254   product constituents that govern volatilization, and the timescale available for these
255   constituents to evaporate. The most notable updates to VCPy include the incorporation of
256   additional product aggregations (e.g., 17 types of industrial coatings), variation in the
257   VOC-content of products to reflect state-level area source rules relevant to the solvent
258   sector, and the adoption of an indoor emissions pathway.

259
260
261   To facilitate calculation of VCP indoor emissions in VCPy, each product category is
262   assigned an indoor usage fraction. All coating and industrial products are assigned a 50%
263   indoor emission fraction, all pesticides and automotive aftermarket products are assigned
264   a 0% indoor emission fraction, and all consumer and cleaning products are assigned a
265   100% indoor emission fraction. The lone exception are daily use personal care products,
266   which are assumed to have a 50% indoor emission fraction. This indoor emission
267   assignment enables the mass transfer coefficient to vary between indoor and outdoor
268   conditions. Typically, the mass transfer coefficient indoors is smaller than the mass
269   transfer coefficient outdoors due to more stagnant atmospheric conditions, and the newest
270   version of the modeling framework reflects these dynamics. Indoor product usage utilizes
271   a mass transfer coefficient of 5 m hr^{-1}, and the remaining outdoor portion is assigned a
272   mass transfer coefficient of 30 m hr^{-1} (Khare and Gentner, 2018; Weschler and Nazaroff,
273   2008). More details about the framework could be found elsewhere (Seltzer et al., 2021).
274   Annual production volumes for different chemical species used in discussion were taken
275   from U.S. EPA's Chemical Data Reporting database (U.S. Environmental Protection
276   Agency, Chemical Data Reporting, 2016).

277

278   **3. Results and discussion**

279   **3.1. Instrument response to diverse chemical functionalities**

280   Of the 1000's of ions observed in the urban ambient mass spectra (Figures 2a, S4) during
281   online sampling with ammonium-adduct ionization, 148 prominent ion signals were
282   targeted for detailed analysis and assigned compound formulas representing a diverse
283   range of chemical functionalities (Table S3). These ions were selected based on high
284   signal-to-noise ratios and likely isomer contributions from VCPs-related emissions. To
285   confirm sensitivity toward these functional groups, the instrument was calibrated using
286   58 analytical standards that are also constituents of various consumer/commercial
287   products. The mass spectrum of individual standards showed high parent ion-to-
288   background signal and negligible fragmentation products (Figure 2a), thus simplifying
289   the interpretation of the soft adduct parent ions in ambient air mass spectra in contrast to
290   higher-fragmentation-prone proton transfer reaction spectra.

291
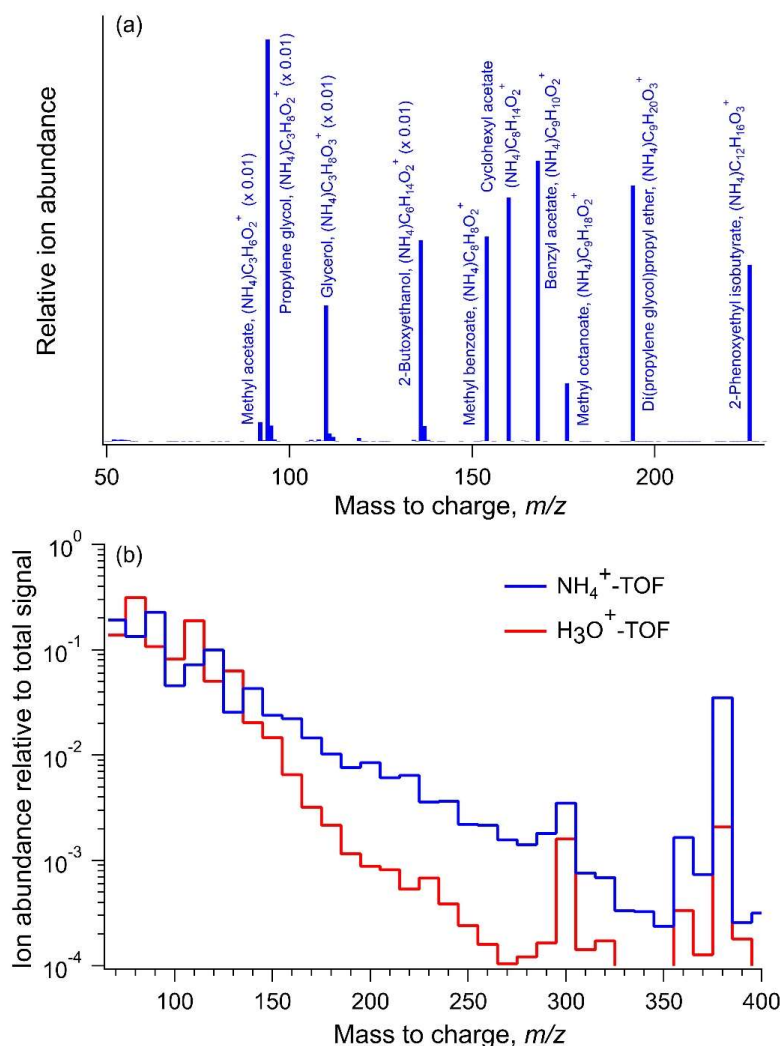
**Figure 2. (a) Negligible parent ion fragmentation (with high signal-to-noise ratios)
across diverse chemical functionalities in CI-ToF allows for measurements of
understudied chemical species (examples from authentic standards shown). (b)
Average ToF mass spectra obtained from NH$_4^+$ and H$_3$O$^+$ (i.e. PTR) ionization
schemes binned over 10 m/z intervals using data from the same Vocus CI-ToF at the
site. The CI-ToF spectra observed greater ion signal in the approximate
intermediate-volatility into the semi-volatile region (e.g., ≥160 m/z). Note: In (b), the
NH$_4^+$ and PTR signals are offset by 18 and 1 m/z respectively to account for the
difference in the mass of the reagent ion and the averages are from different days
when the reagent ion was switched.**

302

303 In laboratory tests with the authentic standards, the instrument showed the highest
304 response factors (i.e. ions ppb^{-1}) toward glycol ethers and ketones (Figure 3). The
305 response factors for most aliphatic and aromatic esters were one order of magnitude
306 smaller than glycol ethers and ketones. Standards for isomers were also run in some cases
307 of possible different compounds contributing to the same ion signal based on multiple
308 prominent compounds estimated in inventories or well-known VCP components. While
309 some isomers elicited similar responses from the instrument, others produced
310 considerably different sensitivities (Figure S5) (Bi et al., 2021). For 7 test cases here, the
311 difference in response factors tended to be most pronounced in the case of isomers with
312 small carbon numbers, e.g. ethyl acetate being 8 times higher than butyric acid, while
313 isomers with larger carbon numbers, e.g. ethylene glycol hexyl ether (EGHE) and 1,2
314 octanediol produced similar ion intensities.

315

316 This variability in instrument response could also depend on other physiochemical
317 properties of the analytes because some acids, e.g. hexadecanoic, fumaric, adipic and
318 salicyclic acids, also responded poorly to calibration. This may be due to poor water
319 solubility in some cases (e.g. adipic and hexadecanoic acid) affecting the calibration
320 mixes, and, also the tendency of lower volatility compounds to partition to surfaces that
321 may reduce their transmission efficiency through the LCS delivery lines and the
322 instrument inlet thus contributing to this marked difference in instrument response
323 between some isomers. Sensitivity analysis showed that the calculated concentrations
324 could have large differences (by a factor of 0.5 to 8) depending on the relative abundance
325 of contributing isomers due to their effect on the overall mass response factor (Figure
326 S5). Hence, in each case where isomers were tested, the mass response factor for the ion
327 was estimated by averaging the instrument response to individual isomers. This can still
328 potentially cause slight over- or under-estimation of ion concentrations in ambient air
329 depending on the relative contribution of isomers to the ion, which is affected by the
330 magnitude of emissions of individual isomers as well as their sources and sinks (e.g.
331 indoor surfaces or reactions).

332

333 The signal intensities could also be influenced by changes in environmental factors such
334 as relative humidity that can modify the relative importance of different ionization
335 pathways in the reaction chamber. However, systematic tests conducted with acetone,
336 methyl ethyl ketone (MEK), acetonitrile and α-pinene found their NH_4^+-adduct signal
337 intensities to be independent of any changes in relative humidity in the CI-ToF ionization
338 region (Figure 1). Thus, day-to-day response factors for individual ions were comparable
339 across the entire sampling period and did not require RH-dependent corrections.
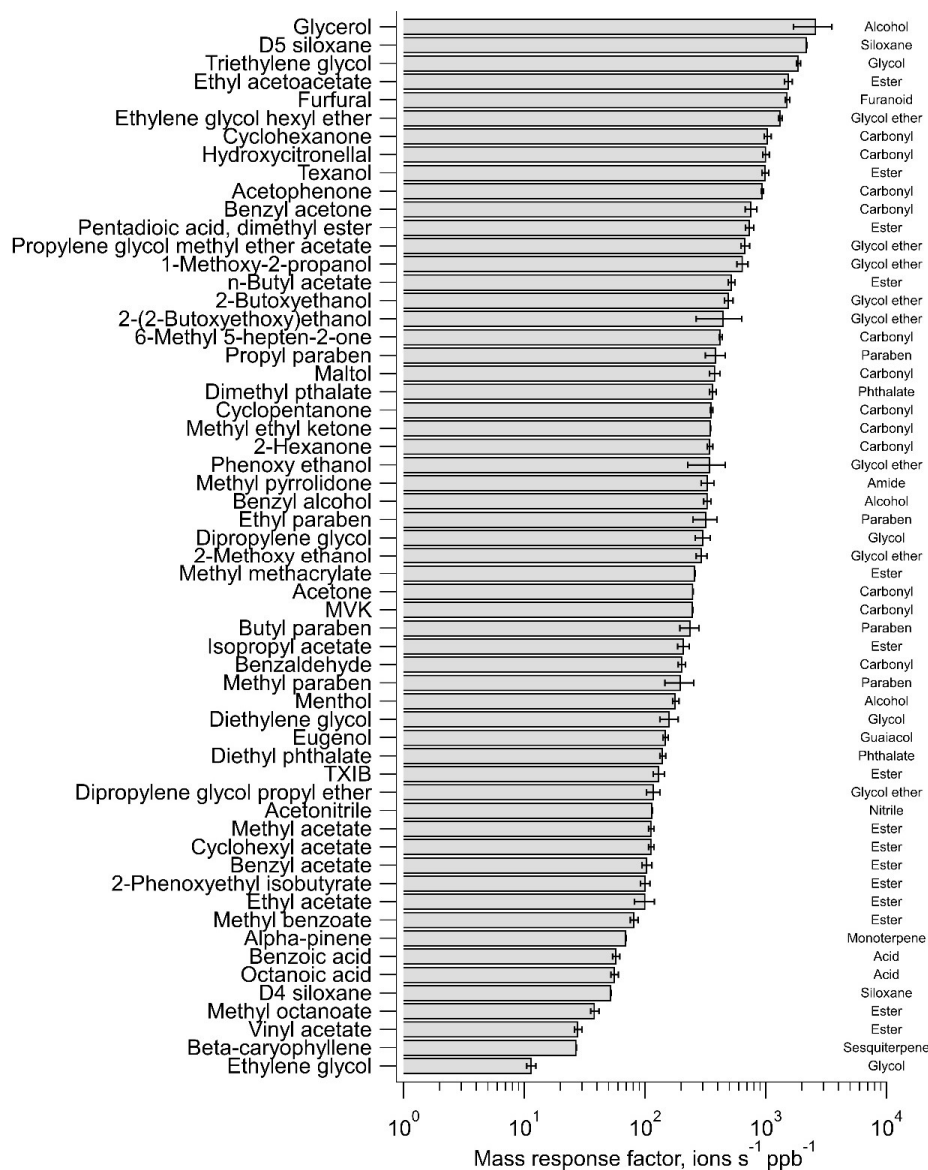
Figure 3. The response of the CI-ToF with NH₄⁺ ionization toward select calibration standards containing a diverse range of chemical functional groups and molecular structures, which are listed (right) for reference, but we note the multi-functionality of some of the compounds.

346   Additionally, the CI-ToF measurements were also validated by comparing the
347   concentration timeseries of some of the OVOCs (i.e. acetone, methyl vinyl ketone
348   (MVK), MEK) and monoterpenes across the entire sampling period with parallel
349   measurements from a co-located PTR-ToF instrument. The measurements largely agreed
350   within 90%, validating the performance of the CI-ToF instrument (Figure S6).

351

352   In case of ion signals that were not quantified, we have carefully considered factors such
353   as annual usage of likely compounds, their atmospheric reactivity and ionization
354   efficiency with the NH_4^+ adduct to inform our discussion of their formula assignments.
355   For example, minimal ethanol ions were observed during instrument calibration
356   suggesting limitations in its detection with NH_4^+ reagent ion. Yet, C_2H_5OH ion signal was
357   measured during ambient sampling. Given the densely urban sampling location, it is
358   likely that this measured C_2H_5OH signal was dimethyl ether that is used in personal care
359   products (propellant) and some potential use as fuel or refrigerant. However, ethanol
360   emissions are still expected to exceed those of dimethyl ether based on the inventories.
361   Similar assessments are made wherever possible in the discussion of temporal trends of
362   uncalibrated ions.

363

364   Vocus CI-ToF captured relatively more ion signal in the 150-350 m/z range (i.e.
365   normalized to the total signal of the mass spectra) when compared with PTR ionization
366   using the same instrument at the same site (Figure 2b). This was due to formation of
367   strongly-bonded NH_4^+-analyte adduct molecules at low collision energies that preserved
368   large functionalized analytes. In comparison, PTR-ToF can strongly fragment certain
369   functionalized analytes (e.g. alcohols) during proton addition rendering interpretation
370   difficult. Hence, we are able to examine a greater diversity of volatile- to semi-volatile
371   functionalized compounds with CI-ToF measurements that are known to be emitted from
372   a wide range of volatile chemical products.

373

374   **3.2 Influence of atmospheric conditions on observed concentrations**

375

376   The concentrations of measured ions varied significantly over the 10-day sampling period
377   influenced by changes in meteorology and dilution, as well as temporal changes in
378   emissions. The concentrations showed clear dependence on wind velocity (4.5 m/s avg.)
379   and direction, indicating variations in both emission rates and dispersion across different
380   areas upwind of the site. The highest concentration signals were observed between 22/1
381   and 25/1 when slower winds (<5 m/s) arrived from the southwest, south, and east across
382   various parts of Manhattan leading up to the site (Figures S2, S7). These areas are
383   characterized by a high population density and include a wide range of commercial
384   activities that could contribute to the concentration enhancements. Additional
385   concentration spikes and smaller enhancements were observed on 27/1 with similar

386 southwesterly winds at higher speeds. Prolonged concentration enhancements were also
387 observed 30/1-31/1 with slower (<5 m/s) winds predominantly from the east, passing
388 over Harlem (Manhattan) after crossing the also densely-populated Bronx with varied
389 commercial/industrial activities. Observed concentrations at the site were lowest with
390 west-northwesterly and northwesterly winds originating from relatively less-densely
391 populated areas, as well as periods of highest wind speeds.

392

393 Concentration trends generally overlapped across all compound classes with a few
394 exceptions (e.g. $C_5H_8O_2$), with variations in their covariances (see Sec. 3.3). This
395 demonstrates a major role for meteorology in determining local VOC concentrations at
396 the site, and elsewhere in NYC. Still in some cases (e.g. nitropropane, 2,5 dimethyl
397 furan), influence of certain short-term sources such as possible local/regional wintertime
398 biomass burning contributions were observed as temporary sharp spikes in compound
399 abundances.

400

401 By influencing the rate of advective transport of pollutants, wind speed also directly
402 impacts the time available for chemical species to undergo oxidation in the atmosphere.
403 Atmospheric oxidation can be an important sink for different chemical species and also a
404 secondary source for some OVOCs (e.g. alcohols, carbonyls) (Franco et al., 2021;
405 Mellouki et al., 2015). Therefore, accounting for their reaction timescales is necessary in
406 the interpretation of their relative abundances. During this sampling campaign, with a
407 local average wind speed of 4.5 m s^{-1} (Figure S7), this translated to 0.5-2 hours of
408 daytime photochemical aging for emissions within 10-30 km of the site (encompassing
409 all of Manhattan, Brooklyn, Queens, the Bronx, and much of urban metro NYC in New
410 Jersey) (Figure S2).

411

412 For species under consideration in this study, the rate constants for reaction with
413 hydroxyl radicals (OH$^{.}$) ranged from 10^{-11} to 10^{-13} molecule^{-1} cm^3 s^{-1} as obtained from the
414 OPERA model and other studies (Aschmann et al., 2001; Mansouri et al., 2018; Picquet-
415 Varrault et al., 2002; Ren et al., 2021). Given wintertime OH concentrations of
416 approximately 10^6 molecules cm^3 in NYC (Ren et al., 2006; Schroder et al., 2018), this
417 puts their daytime atmospheric lifetimes (i.e. e-folding times) between 1-2 days to several
418 months with some variation with OH concentrations. For average wind speeds observed
419 during sampling, this translated to daytime concentration losses of 10% or less for the
420 vast majority of measured species if emitted within a distance of 10-15 kilometers of the
421 site (Figure S8), which includes all of Manhattan and other densely populated areas of
422 New York City and adjacent New Jersey (Figure S2). For future work at the site, we note

423   that daytime OH concentrations in NYC during summer will be higher (e.g. five times the

424   winter values in NYC, (Ren et al., 2006)), which can affect the interpretation of source

425   contributions to more reactive chemical species with shorter lifetimes. The other

426   important daytime oxidant ozone is not likely to react significantly in the absence of non-

427   aromatic unsaturated C=C bonds in most targeted ions in this study (de Gouw et al.,

428   2017), especially during the winter. The k values for nighttime oxidation with the nitrate

429   radicals are 1 to 4 orders of magnitude smaller ($\sim 10^{-12}$-10^{-15} molecule^{-1} cm^3 s^{-1}) with

430   average NO_3 concentrations on the order of 10^8 molecules cm^{-3} (Asaf et al., 2010; Cao et

431   al., 2018). Thus, nighttime oxidation is not likely to lead to shorter VOC lifetimes than

432   those calculated for daytime OH oxidation. In all, it is unlikely that the emissions of the

433   target compounds in this study were substantially influenced by oxidative losses in the

434   ambient atmosphere, and were predominantly driven by the magnitude of emissions in

435   NYC and their atmospheric dilution. Yet, the observed ambient concentrations of

436   different species could be potentially affected by the extent of their indoor vs. outdoor

437   usage, seasonal patterns in applications (e.g., wintertime outdoor use of ethylene glycol

438   as antifreeze), or physical processes related to their sources or sinks (e.g. partitioning).

439

440

441   **3.3. Ambient measurements across diverse chemical classes**

442   Within the broader distribution of ion signals across the entire ambient mass spectra, we

443   identified a diversity of chemical species. A selection of the most prominent ions in

444   various compound categories are discussed in this section. Table S4 summarizes different

445   use sectors, but the vast majority have uses in personal care products, fragrances, a wide

446   range of solvents, and/or other volatile consumer products. As such, some of the most

447   abundant ions observed here were related to compounds found in the formulations of

448   these types of products and/or had large annual production volumes (U.S. Environmental

449   Protection Agency, Chemical Data Reporting, 2016). For some volatile compounds that

450   exhibited low atmospheric abundances despite large annual production, it is possible that

451   a substantial fraction of the production volume goes as feedstock to manufacture

452   derivatives or are otherwise not prone to gas-phase emissions. Yet, seasonal differences

453   in use, partitioning to the gas phase, and/or indoor-to-outdoor transport could also

454   contribute to potential inter-annual variations.

455

456   The ions above 100 parts per trillion (ppt) on average included those with contributions

457   from acetates, C_2H_6O (e.g. ethylene glycol), C_3H_6O (e.g. acetone), C_2H_3N (e.g.

458   acetonitrile), $C_{10}H_{16}$ (e.g. monoterpenes), C_4H_8O (e.g. methyl ethyl ketone) and $C_5H_8O_2$

459   (e.g. methyl methacrylate) (Table 1). A detailed discussion of the trends in concentrations

460   and ion abundances of these and other ions is presented below and separated into distinct

461   categories based on chemical class or use-type.

462 **Table 1. List of ions calibrated with authentic standards (Table S2), probable**
463 **contributing isomers, geometric mean concentrations (with standard deviations),**
464 **annual emissions in each inventory, and mean concentration enhancement ratios**
465 **(with standard deviations of the mean and linear correlation coefficients) with**
466 **acetone and other prominent combustion-related tracers. Isomer identifications**
467 **marked with asterisks (*) were confirmed in offline GC-EI-MS measurements, with**
468 **additional possible isomers included in Table S4.**

Compound formula, i	Probable compounds, i	Geo. mean concentration, ppt, i	Emissions, kg yr⁻¹ VCPy, FIVE-VCP	Ratios to tracer compounds (Δmol/Δmol) [†]			
				$\Delta i/\Delta$Benzene (r)	$\Delta i*1000/\Delta$CO (r)	$\Delta i/\Delta$Acetone (r)	$\Delta i/\Delta$Benzyl alcohol (r)
$C_2H_6O_2$	Ethylene glycol	2437±3622	361511, 260540	1.1E+01±1.7E+00 (0.79)	9.1E+00±1.3E+00 (0.83)	2.8E+00±4.3E-01 (0.95)	3.0E+02±4.2E+01 (0.88)
C_3H_6O	Acetone*	977±783	1333642, 1647548	3.8E+00±4.8E-01 (0.83)	3.3E+00±3.7E-01 (0.87)	--	1.1E+02±1.1E+01 (0.92)
$C_4H_6O_2$	Methyl acrylate*, Diacetyl*	810±396	1905, 4638	2.1E+00±2.5E-01 (0.82)	1.8E+00±1.9E-01 (0.89)	5.6E-01±6.1E-02 (0.95)	5.9E+01±5.6E+00 (0.94)
$C_4H_8O_2$	Ethyl acetate*, Butyric acid	679±664	27958, 323	2.8E+00±3.6E-01 (0.72)	2.3E+00±2.8E-01 (0.73)	7.2E-01±8.9E-02 (0.73)	7.6E+01±8.5E+00 (0.67)
$C_3H_6O_2$	Methyl acetate*, Propionic acid, Hydroxyacetone, Ethyl formate	435±377	50747, 114453	1.7E+00±2.2E-01 (0.64)	1.5E+00±1.6E-01 (0.65)	4.5E-01±5.3E-02 (0.76)	4.8E+01±5.0E+00 (0.7)
C_2H_3N	Acetonitrile	246±102		8.5E-01±9.0E-02 (0.32)	7.2E-01±6.4E-02 (0.24)	2.2E-01±2.2E-02 (0.35)	2.3E+01±1.9E+00 (0.33)
$C_{10}H_{16}$	Monoterpenes (e.g., limonene*, α-Pinene*)	156±105	60206, 17107	5.1E-01±6.5E-02 (0.79)	4.3E-01±4.9E-02 (0.87)	1.3E-01±1.6E-02 (0.85)	1.4E+01±1.5E+00 (0.94)
C_4H_8O	MEK, THF, Cyclopropyl carbinol*	126±82	41369, 293752	4.3E-01±5.1E-02 (0.79)	3.7E-01±3.8E-02 (0.84)	1.1E-01±1.2E-02 (0.93)	1.2E+01±1.1E+00 (0.85)
$C_5H_{10}O_2$	Isopropyl acetate*, n-propyl acetate*	114±106	2845, 5831	4.4E-01±5.7E-02 (0.61)	3.7E-01±4.4E-02 (0.69)	1.1E-01±1.4E-02 (0.69)	1.2E+01±1.3E+00 (0.58)
$C_5H_8O_2$	Methyl methacrylate*	108±121	1102, -	4.1E-01±6.0E-02 (0.45)	3.5E-01±4.7E-02 (0.37)	1.1E-01±1.5E-02 (0.5)	1.1E+01±1.5E+00 (0.41)
$C_6H_{12}O_2$	Butyl acetate*	103±138	74432, 62692	4.9E-01±6.9E-02 (0.76)	4.1E-01±5.4E-02 (0.77)	1.3E-01±1.7E-02 (0.87)	1.3E+01±1.7E+00 (0.83)
$C_8H_8O_2$	Methyl benzoate*	92±15		1.1E-01±1.2E-02 (0.72)	9.1E-02±8.4E-03 (0.75)	2.8E-02±2.8E-03 (0.78)	3.0E+00±2.5E-01 (0.79)
$C_8H_{16}O_2$	Caprylic acid* (i.e., Octanoic acid), hexyl acetate	87±47	5281, -	2.5E-01±2.9E-02 (0.81)	2.1E-01±2.2E-02 (0.92)	6.5E-02±7.2E-03 (0.92)	6.9E+00±6.6E-01 (0.95)
$C_3H_8O_2$	2-Methoxy ethanol, propylene glycol*	82±51	240692, -	2.9E-01±3.3E-02 (0.71)	2.4E-01±2.4E-02 (0.71)	7.5E-02±8.0E-03 (0.85)	7.9E+00±7.3E-01 (0.77)
$C_9H_{18}O_2$	Methyl octanoate, Nonanoic acid*	77±24		1.4E-01±1.6E-02 (0.79)	1.2E-01±1.2E-02 (0.9)	3.7E-02±3.9E-03 (0.9)	3.9E+00±3.5E-01 (0.94)
C_7H_6O	Benzaldehyde*	76±37	142, 2	2.1E-01±2.5E-02 (0.83)	1.8E-01±1.8E-02 (0.88)	5.4E-02±6.1E-03 (0.88)	5.7E+00±5.6E-01 (0.93)
$C_{15}H_{24}$	Sesquiterpenes (e.g., β-Caryophyllene)	70±11		7.3E-02±8.3E-03 (0.73)	6.2E-02±6.1E-03 (0.83)	1.9E-02±2.0E-03 (0.78)	2.0E+00±1.8E-01 (0.9)
$C_6H_{12}O$	2-Hexanone*, 4-Methyl-2-pentanone	59±42	6162, 16527	2.0E-01±2.5E-02 (0.83)	1.7E-01±1.9E-02 (0.84)	5.3E-02±6.1E-03 (0.92)	5.6E+00±5.7E-01 (0.91)
$C_7H_6O_2$	Benzoic acid*	59±9		5.8E-02±6.3E-03 (0.48)	4.9E-02±4.6E-03 (0.39)	1.5E-02±1.5E-03 (0.4)	1.6E+00±1.4E-01 (0.45)
C_4H_6O	MVK, MACR	58±39		1.9E-01±2.4E-02 (0.83)	1.6E-01±1.8E-02 (0.87)	4.9E-02±5.9E-03 (0.94)	5.1E+00±5.5E-01 (0.94)
$C_8H_{14}O_2$	Cyclohexyl acetate	43±20		1.2E-01±1.4E-02 (0.81)	1.0E-01±1.0E-02 (0.89)	3.2E-02±3.4E-03 (0.95)	3.4E+00±3.0E-01 (0.95)
$C_9H_{10}O_2$	Benzyl acetate	39±19	7, -	1.0E-01±1.2E-02 (0.82)	8.8E-02±9.0E-03 (0.89)	2.7E-02±3.0E-03 (0.87)	2.9E+00±2.7E-01 (0.95)
$C_6H_{14}O_3$	Dipropylene glycol	36±28	41085, 116574	1.4E-01±1.7E-02 (0.65)	1.2E-01±1.3E-02 (0.71)	3.6E-02±4.1E-03 (0.7)	3.8E+00±3.8E-01 (0.8)
$C_4H_{10}O_3$	Diethylene glycol	32±17	7026, 122315	8.9E-02±1.1E-02 (0.84)	7.5E-02±7.9E-03 (0.87)	2.3E-02±2.6E-03 (0.91)	2.4E+00±2.4E-01 (0.92)
$C_{10}H_{20}O$	Menthol, Decanal*	31±18	971, 0.06	9.4E-02±1.1E-02 (0.77)	7.9E-02±8.2E-03 (0.89)	2.4E-02±2.7E-03 (0.9)	2.6E+00±2.5E-01 (0.96)
C_5H_8O	Cyclopentanone	30±16		8.4E-02±9.8E-03 (0.84)	7.1E-02±7.2E-03 (0.9)	2.2E-02±2.4E-03 (0.95)	2.3E+00±2.2E-01 (0.95)
$C_6H_{14}O_2$	2-Butoxyethanol*, 1-propoxy-2-propanol*	23±19	107758, 79520	8.9E-02±1.1E-02 (0.8)	7.5E-02±8.2E-03 (0.87)	2.3E-02±2.7E-03 (0.91)	2.4E+00±2.5E-01 (0.91)
$C_8H_{24}O_4Si_4$	D4 siloxane*	23±3	12872, 102213	2.3E-02±2.5E-03 (0.38)	2.0E-02±1.8E-03 (0.48)	6.0E-03±6.1E-04 (0.48)	6.4E-01±5.5E-02 (0.59)
$C_{16}H_{30}O_4$	TXIB*	18±4	- , 2496	2.6E-02±3.0E-03 (0.73)	2.2E-02±2.2E-03 (0.83)	6.8E-03±7.2E-04 (0.75)	7.2E-01±6.5E-02 (0.86)

Formula	Name						
$C_{10}H_{12}O_2$	Eugenol	16±5	45, -	3.1E-02±3.5E-03 (0.82)	2.6E-02±2.5E-03 (0.85)	7.9E-03±8.4E-04 (0.91)	8.4E-01±7.6E-02 (0.92)
$C_9H_{20}O_3$	Dipropylene glycol propyl ether	16±4	4150, 6578	2.3E-02±2.7E-03 (0.65)	2.0E-02±2.0E-03 (0.71)	6.1E-03±6.5E-04 (0.62)	6.4E-01±5.9E-02 (0.73)
$C_{12}H_{16}O_3$	2-Phenoxyethyl isobutyrate	16±2		1.6E-02±1.7E-03 (0.73)	1.3E-02±1.2E-03 (0.76)	4.1E-03±4.1E-04 (0.79)	4.4E-01±3.6E-02 (0.83)
$C_{10}H_{30}O_5Si_5$	D5 siloxane*	16±15	272778, 357202	6.7E-02±8.5E-03 (0.7)	5.7E-02±6.4E-03 (0.82)	1.7E-02±2.1E-03 (0.82)	1.8E+00±2.0E-01 (0.9)
$C_{12}H_{14}O_4$	Diethyl phthalate*	15±3	17138, -	2.3E-02±2.4E-03 (0.64)	1.9E-02±1.7E-03 (0.7)	5.9E-03±5.8E-04 (0.65)	6.2E-01±5.1E-02 (0.71)
C_7H_8O	Benzyl alcohol	14±6	22898, 22923	3.6E-02±4.1E-03 (0.85)	3.1E-02±3.0E-03 (0.92)	9.5E-03±1.0E-03 (0.92)	--
$C_8H_{14}O$	6-Methyl 5-hepten-2-one	14±7		4.1E-02±4.6E-03 (0.81)	3.4E-02±3.4E-03 (0.89)	1.1E-02±1.1E-03 (0.96)	1.1E+00±1.0E-01 (0.96)
$C_8H_8O_3$	Methyl paraben	14±4		2.4E-02±2.7E-03 (0.83)	2.1E-02±2.0E-03 (0.86)	6.3E-03±6.6E-04 (0.83)	6.7E-01±6.0E-02 (0.87)
$C_4H_{10}O_2$	1-Methoxy-2-propanol*	13±8	3405, 2405	4.1E-02±4.9E-03 (0.78)	3.5E-02±3.6E-03 (0.85)	1.1E-02±1.2E-03 (0.89)	1.1E+00±1.1E-01 (0.89)
$C_5H_4O_2$	Furfural*	13±6	- , 0.01	3.4E-02±4.0E-03 (0.71)	2.9E-02±2.9E-03 (0.62)	8.8E-03±9.7E-04 (0.56)	9.3E-01±8.9E-02 (0.66)
$C_6H_{10}O$	Cyclohexanone	12±6	384, 106653	3.6E-02±4.1E-03 (0.84)	3.0E-02±3.0E-03 (0.91)	9.4E-03±1.0E-03 (0.96)	9.9E-01±9.1E-02 (0.92)
$C_6H_{12}O_3$	PGMEA*, 2-Ethoxyethyl acetate	12±11	10017, 8214	4.7E-02±6.0E-03 (0.78)	4.0E-02±4.6E-03 (0.76)	1.2E-02±1.5E-03 (0.9)	1.3E+00±1.4E-01 (0.86)
$C_6H_6O_3$	Maltol	11±3		1.3E-02±1.6E-03 (0.59)	1.1E-02±1.2E-03 (0.44)	3.4E-03±3.8E-04 (0.42)	3.6E-01±3.5E-02 (0.49)
C_8H_8O	Acetophenone*	10±6	4, -	3.2E-02±3.8E-03 (0.81)	2.7E-02±2.9E-03 (0.85)	8.4E-03±9.4E-04 (0.89)	8.8E-01±8.7E-02 (0.9)
C_5H_9NO	Methyl pyrrolidone	9±3	12749, 15452	1.9E-02±2.2E-03 (0.72)	1.6E-02±1.6E-03 (0.78)	5.0E-03±5.3E-04 (0.77)	5.3E-01±4.8E-02 (0.78)
$C_8H_{10}O_2$	Phenoxyethanol*	9±3	9851, 0.25	1.7E-02±2.0E-03 (0.78)	1.5E-02±1.5E-03 (0.84)	4.5E-03±4.9E-04 (0.86)	4.8E-01±4.4E-02 (0.91)
$C_8H_{18}O_3$	2-(2-Butoxyethoxy)ethanol, DGBE	8±4	48389, 68370	2.1E-02±2.4E-03 (0.85)	1.8E-02±1.8E-03 (0.91)	5.4E-03±5.9E-04 (0.89)	5.7E-01±5.4E-02 (0.94)
$C_{10}H_{10}O_4$	Dimethyl phthalate	7±1	70, -	9.1E-03±1.0E-03 (0.62)	7.7E-03±7.4E-04 (0.62)	2.4E-03±2.5E-04 (0.55)	2.5E-01±2.2E-02 (0.65)
$C_{12}H_{24}O_3$	Texanol*	7±4	267615, 197658	2.0E-02±2.4E-03 (0.57)	1.7E-02±1.8E-03 (0.74)	5.3E-03±5.9E-04 (0.67)	5.6E-01±5.5E-02 (0.74)
$C_9H_{10}O_3$	Ethyl paraben	6±1		7.0E-03±7.7E-04 (0.84)	5.9E-03±5.6E-04 (0.84)	1.8E-03±1.9E-04 (0.85)	1.9E-01±1.7E-02 (0.9)
$C_{11}H_{14}O_3$	Butyl paraben	6±1		8.5E-03±9.0E-04 (0.71)	7.2E-03±6.5E-04 (0.74)	2.2E-03±2.2E-04 (0.8)	2.3E-01±1.9E-02 (0.76)
$C_6H_{10}O_3$	Ethyl acetoacetate	4±2		1.3E-02±1.5E-03 (0.85)	1.1E-02±1.1E-03 (0.87)	3.4E-03±3.7E-04 (0.93)	3.6E-01±3.4E-02 (0.91)
$C_{10}H_{12}O$	Benzyl acetone	4±2		1.0E-02±1.2E-03 (0.85)	8.5E-03±8.8E-04 (0.91)	2.6E-03±2.9E-04 (0.94)	2.8E-01±2.6E-02 (0.97)
$C_7H_{12}O_4$	Pentadioic acid, dimethyl ester	4±1	4942, 28232	7.2E-03±8.0E-04 (0.8)	6.1E-03±5.8E-04 (0.84)	1.9E-03±1.9E-04 (0.87)	2.0E-01±1.7E-02 (0.89)
$C_{10}H_{12}O_3$	Propyl paraben	4±1		6.3E-03±7.1E-04 (0.54)	5.3E-03±5.3E-04 (0.46)	1.6E-03±1.7E-04 (0.42)	1.7E-01±1.6E-02 (0.51)
$C_{10}H_{20}O_2$	Hydroxycitronellal	3±1		5.3E-03±5.9E-04 (0.78)	4.5E-03±4.3E-04 (0.88)	1.4E-03±1.4E-04 (0.92)	1.5E-01±1.3E-02 (0.95)
$C_8H_{18}O_2$	Ethylene glycol hexyl ether*, 1,2-Octanediol	2±1	15836, 8544	5.8E-03±6.7E-04 (0.8)	4.9E-03±4.9E-04 (0.88)	1.5E-03±1.6E-04 (0.87)	1.6E-01±1.5E-02 (0.94)
$C_3H_8O_3$	Glycerol	1±0.5	148441, 1046753	3.0E-03±3.5E-04 (0.66)	2.6E-03±2.5E-04 (0.69)	7.9E-04±8.4E-05 (0.75)	8.3E-02±7.6E-03 (0.74)
$C_6H_{14}O_4$	Triethylene glycol	1±0.3	1718, 1053	2.1E-03±2.4E-04 (0.47)	1.8E-03±1.7E-04 (0.45)	5.5E-04±5.8E-05 (0.4)	5.8E-02±5.2E-03 (0.51)

469 † Note: For comparison to the emissions inventories, the standard deviation of the mean was used for the compound ratios to constrain
470 the uncertainty of the average compound ratios over the 10-day period, yet we note that higher time resolution variations in the
471 observed ratios are expected given the spatiotemporal variations in emissions from contributing sources distributed around the site.
472 Given the varied correlation coefficients against tracers (Figure 6), to reduce bias, background-subtracted geometric means are used to
473 determine the compound ratios, though the geometric mean ratios and slopes are similar, especially for well-correlated compound
474 pairs (Figure S11).

475

3.3.1 Esters

477 Prominent esters observed in this study and discussed here include acetates and acrylates.
478 $C_3H_6O_2$, $C_4H_6O_2$, $C_4H_8O_2$, $C_5H_{10}O_2$ and $C_6H_{12}O_2$ were ions with some of the highest
479 ambient concentrations in our data whose geometric mean concentrations varied between

480   0.1-0.8 ppb (Figure 4a-f). Small acetates (e.g. methyl-, ethyl-, propyl- and butyl- acetates)
481   are likely major contributors to these ion signals since they are being extensively used as
482   oxygenated solvents and contribute to natural and designed fragrances/flavorings. The
483   VCPy model estimates the annual emissions of these acetates to be on the order of 10^4-
484   10^5 kg yr^{-1} in NYC, but other compounds can also contribute to these ions. For example,
485   hydroxyacetone and propionic acid may add to $C_3H_6O_2$, diacetyl and γ-butyrolactone to
486     $C_4H_6O_2$, methyl propionate and butyric acid to $C_4H_8O_2$, isobutyl formate to $C_5H_{10}O_2$, and,
487   diacetone alcohol and methyl pentanoate to $C_6H_{10}O_2$. However, their estimated emissions
488   are 1-2 orders of magnitude smaller than each of the acetates, likely making them minor
489   contributors to observed ion intensities. $C_8H_{14}O_2$ (e.g. cyclohexyl acetate) and $C_9H_{10}O_2$
490   (e.g. benzyl acetate) were also important ions within this category with average
491   concentrations at 40 ± 20 ppt and peaks reaching up to 150 ppt during the measurement
492   period.

493

494   We observed hourly $C_5H_8O_2$ concentrations exceeding 1 ppb (Figure 5), which includes
495   methyl methacrylate (MMA) and potential contributions from 2,3-pentanedione and ethyl
496   acrylate given their use as solvents in various coatings and inks. MMA sees some use in
497   adhesives, paints and safety glazing (estimated emissions ~10^3 kg yr^{-1}; VCPy), but could
498   also potentially be emitted from the common polymer poly-(methyl methacrylate)
499   (PMMA) which is used in plastic materials. With a geometric mean concentration of 100
500     $\pm$ 120 ppt, possible contributions of PMMA offgassing/degradation as a source of
501   ambient MMA warrants further investigation, but has been observed in polymer studies
502   (Bennet et al., 2010). In addition to isomer-specific observations of MMA, we note that
503   most of the acetates were also confirmed via offline measurements using adsorbent tubes
504   that were analyzed using GC EI-MS for compound-specific identification (Table 1).

505
506
507   **3.3.2 Carbonyls**
508
509   Carbonyls are also extensively used as replacements for non-polar solvents in various
510   consumer/commercial applications along with use in cosmetics and personal care
511   products. Hence, C_3H_6O (e.g. acetone), C_4H_8O (e.g. methyl ethyl ketone) and $C_6H_{12}O$
512   (e.g. methyl butyl ketone) were expectedly present at relatively high concentrations.
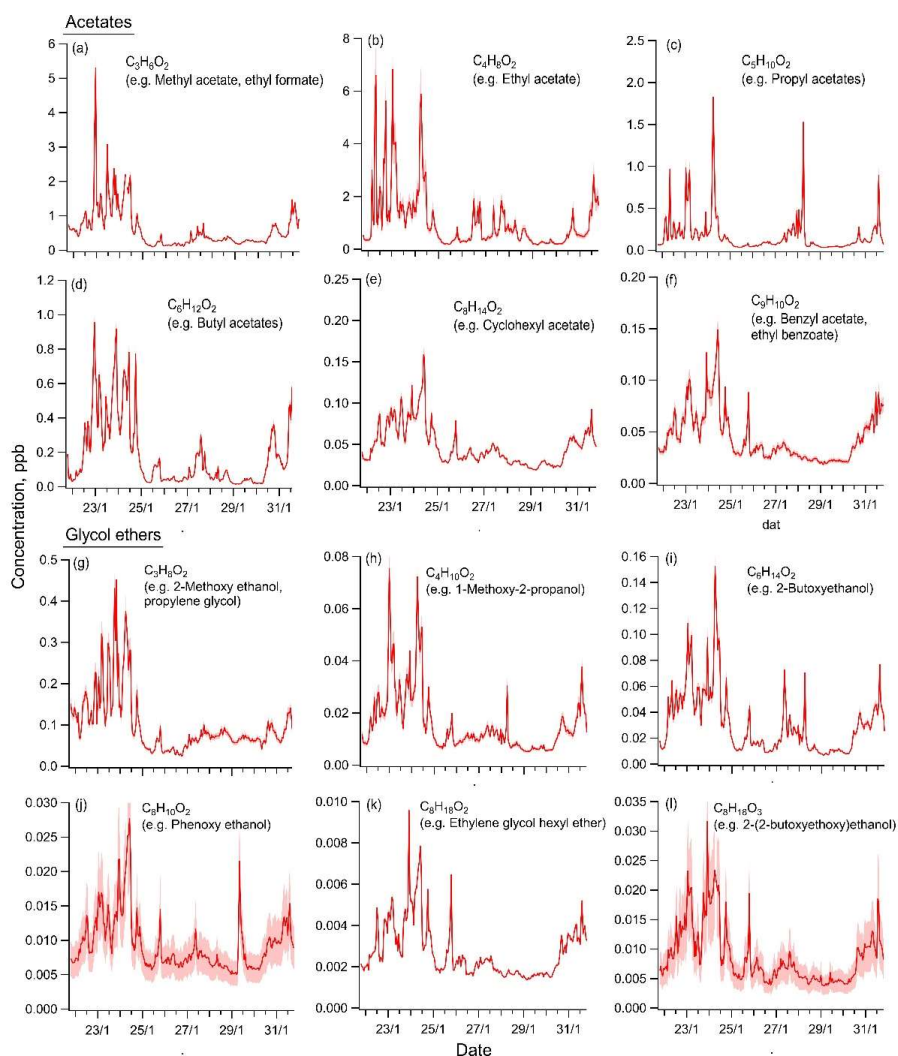
Figure 4. **The concentration timeseries of select, widely-used acetates and glycol ethers. Timeseries are shown with major isomers as examples with a more comprehensive list available in Tables 1 and S4. Displayed uncertainty bands are a function of calibration uncertainties (including for isomer pairs).**

Given the absence of considerable known emissions of isomers, the ion intensities were mainly attributed to these carbonyl compounds. Acetone showed the highest average concentrations in urban air among all carbonyl solvents detected (Table 1). Since biogenic and secondary sources of acetone (i.e. from atmospheric oxidation) are

523   relatively limited in NYC wintertime conditions, the measurements are consistent with

524   very high anthropogenic emissions in NYC (~10^6 kg yr^{-1}) and extensive use in products

525   and by industries (~10^9 kg yr^{-1} nationwide).

526
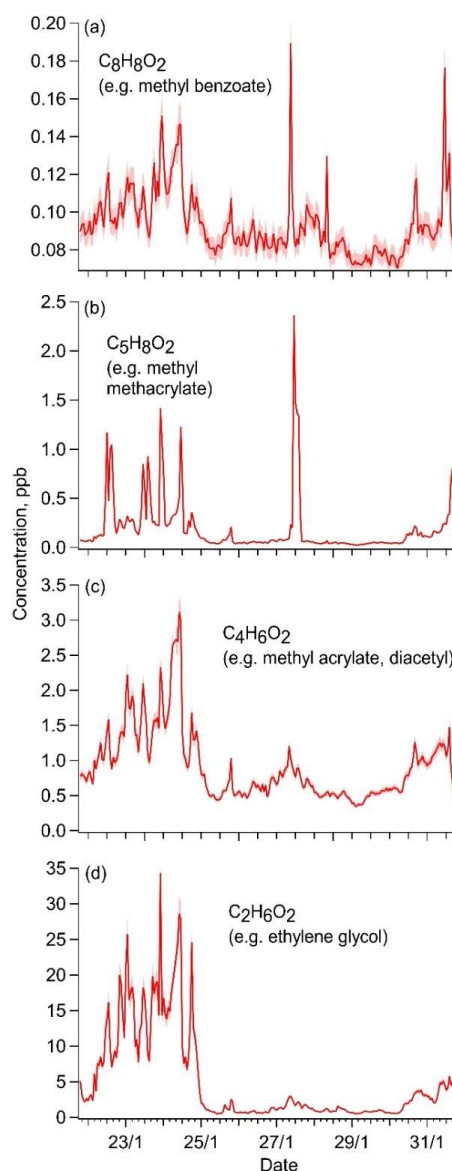
Figure 5. Concentration timeseries of select prominent ions that include contributions from major VCP-related compounds (examples listed; see Tables 1 and S4 for expanded list).

530

531   MEK was the second highest carbonyl observed with C_4H_8O ion concentration spanning
532   from 50 to over 500 ppt. Its estimated emissions are 0.4-3 $\times10^5$ kg yr^{-1} or greater in NYC
533   and it finds significant use in coatings with large annual nationwide consumption (~10^8
534   kg yr^{-1}). Methyl butyl ketone (MBK) and cyclohexanone were the next most abundant in
535   this category. The average concentration of MBK at 58 ± 42 ppt was nearly 50% of MEK
536   but reached up to 300 ppt during the initial 4 days of the sampling period. Cyclohexanone
537   however was much smaller at 12 ± 7 ppt with highest concentrations reaching up to only
538   35 ppt across the measurement period, which was consistent with its emissions in VCPy
539   (~400 kg yr^{-1}) being at least two orders of magnitude smaller than other species in this
540   category, though its estimated emissions in FIVE-VCP were much higher (Table 1).

541
542

3.3.3 Glycols and glycol ethers

544   Glycols and glycol ethers are compound classes that have been traditionally challenging
545   to measure in real-time with PTR-ToF instruments, being prone to ionization-induced
546   fragmentation during online sampling. With Vocus CI-ToF, we were able to measure
547   signals of several glycol and glycol ether compounds. The most prominent ones included
548   C_2H_6O, $C_3H_8O_2$, $C_6H_{14}O_2$ and $C_4H_{10}O_2$ ions whose concentrations ranged between 10-500
549   ppt across the sampling period (Figure 4g-l) with C_2H_6O reaching ppb-levels.

550

551   $C_2H_6O_2$ (e.g. ethylene glycol) was the most abundant observed compound in this study
552   (Table 1). The emissions of ethylene glycol in NYC are estimated to be on the order of 3-
553   4×10^5 kg yr^{-1} which is a factor of 3 smaller than acetone (~10^6 kg yr^{-1}; VCPy and FIVE-
554   VCP). Still the mean concentration of $C_2H_6O_2$ (2.4 ± 3.6 ppb) was found to be
555   considerably larger than that of C_3H_6O (0.95 ± 0.73 ppb). This difference in their relative
556   ratio could not be explained by their atmospheric lifetimes since ethylene glycol is
557   estimated to be considerably shorter lived than acetone (1.5 vs 33 days).

558

559   The $C_3H_8O_2$ ion (20-450 ppt) likely represented propylene glycol, which was the highest
560   emitted isomer in NYC (~10^5 kg yr^{-1}; VCPy and FIVE-VCP) estimates with
561   comparatively minor contributions from 2-methoxy ethanol and dimethoxymethane, all
562   of which are used as solvents in varnishes and various cosmetics. $C_6H_{14}O_2$, including 2-
563   butoxyethanol, a coupling agent in water-based coatings as well as solvent in varnishes,
564   inks, cleaning products and resins, was observed at 10-150 ppt. The estimated emissions
565   of isomer hexylene glycol are 100 times smaller and would likely not have contributed
566   much to the $C_6H_{14}O_2$ ion signal.

567

568    $C_4H_{10}O_2$, which ranged 10-80 ppt, includes 1-methoxy-2-propanol and 2-ethyoxyethanol
569   as both are used as organic solvents in industrial and commercial applications. Based on
570   emissions estimates, 1-methoxy-2-propanol is expected to be the dominant contributor to
571   this signal with NYC emissions of ~2-3x10^3 kg yr^{-1}, which are 30-50 times higher than 2-
572   ethoxyethanol in estimates. $C_6H_{12}O_3$ varied over a similar concentration range (5-80 ppt)
573   resulting from propylene glycol methyl ether acetate (a.k.a. PGMEA) emissions (~0.7-
574   1x10^4 kg yr^{-1}). The estimated emissions of the other likely isomer, 2-ethoxyethyl acetate,
575   were lower by a factor of 100. Relatively smaller concentrations of $C_8H_{10}O_2$, $C_8H_{18}O_2$
576   and $C_8H_{18}O_3$ ranging between 2-30 ppt were also observed (Figure 4j-l) which include
577   glycol ethers based on their higher emissions relative to other isomers.

578
579
580   ### 3.3.4 Select compounds related to personal care products
581
582   Many personal care products routinely include D5 which is often used as a tracer for
583   emissions from this source category (Gkatzelis et al., 2021a). Hence, we attributed all of
584   the measured $C_{10}H_{30}O_5Si_5$ ion abundance to D5 in this study. Both the VCPy and FIVE-
585   VCP inventories estimate the annual emissions of D5 to be slightly higher (~10^5 kg yr^{-1})
586   than common oxygenated solvents, e.g. esters. However, its ambient concentration was
587   found to be much lower in comparison to them and other oxygenated solvents, varying
588   from 10 ppt to 140 ppt during the 10-day period with a geometric mean of 16 ppt. Other
589   studies report similar concentrations in U.S. cities (Coggon et al., 2018; Stockwell et al.,
590   2021). Compared to the emissions inventories, ambient concentrations were lower by a
591   factor of 2, potentially due to wintertime conditions (e.g. partitioning), the relative
592   amount emitted indoors vs outdoors, and/or limitations in indoor-to-outdoor transport.
593   The distinct enhancement in ambient concentrations of D5 in the morning and evening
594   hours in incoming winds over Manhattan indicated that people were a dominant
595   emissions pathway of D5 emissions in NYC. Since most people spend majority of their
596   day indoors, D5 emissions are subjected to large indoor sinks thereby dampening their
597   contribution to outdoors and will likely be sensitive to reduced wintertime ventilation
598   (Sheu et al., 2021; Wang et al., 2020). By comparison, while estimated emissions of
599   benzyl alcohol in NYC were only ~20% of D5, it had similar average concentrations as
600   D5 (Table 1) ranging from 8 to 40 ppt. With strong correlations with many VCP-related
601   compounds (Figure 6), wide use in various consumer product formulations and a similar
602   kOH to m-xylene (i.e., ~10^{-11} molecule^{-1} cm3 s^{-1}), this suggests its potential as an
603   additional VCP compound for routine monitoring/analysis.

604

605   The glycerol-related $C_3H_8O_3$ ion was especially interesting. Only 1-7 ppt was detected
606   across the measurement period even though it is widely used in the personal care industry
607   with estimated annual emissions in NYC on the order of 10^5 kg yr^{-1}. However, Li et al

608   show in a laboratory evaporation study that glycerol evaporation is much slower than

609   expected (Li et al., 2018). Still, glycerol is expected to influence air quality based on its

610   projected emissions (Gkatzelis et al., 2021b) and no other isomers exist with significant

611   known emissions. Yet, the ratio of background-subtracted concentrations of $C_3H_8O_3$ to

612   D5 ($\Delta C_3H_8O_3/\Delta D5$) was 0.042 despite a much higher ratio of estimated emissions (2, 12

613   mol/mol: VCPy, FIVE-VCP). This suggests that $C_3H_8O_3$ is significantly lower than

614   would be expected based on D5-related activities, and, potentially points to limitations in

615   evaporation, indoor-to-outdoor transport, or atmospheric partitioning—all of which could

616   be influenced by wintertime conditions.
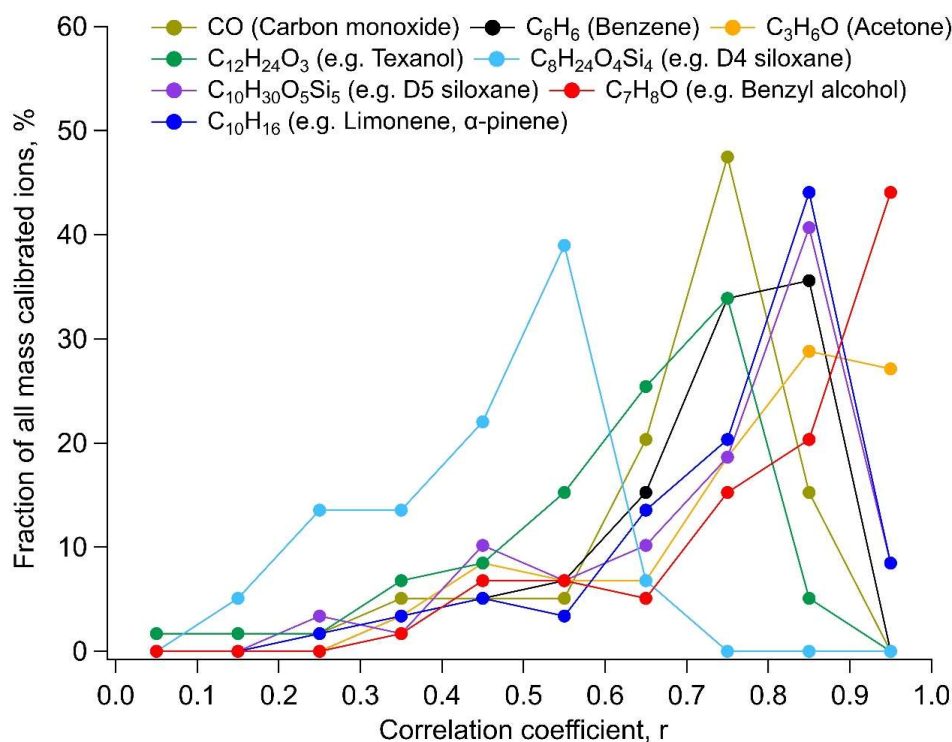
617

618   **Figure 6. A comparison of correlations to major tracer compounds. Distributions of**

619   **correlation coefficients (using hourly-average data) for Table 1 compounds against**

620   **select prominent compounds used as markers of VCP-related sources or general**

621   **anthropogenic emissions (e.g. CO, benzene). Results binned into 0.1 intervals; for**

622   **example, ~45% of compounds were highly-correlated at $0.9 < r < 1$ with C_7H_8O (i.e.**

623   **benzyl alcohol). See SI for similar analysis including all uncalibrated target ions and**

624   **correlation comparisons for all target compounds (Figures S12-15, S17).**

625

$C_8H_8O_3$, $C_9H_{10}O_3$, $C_{10}H_{12}O_3$ and $C_{11}H_{14}O_3$ are paraben-related ions, but additional isomers (e.g. p-ethoxybenzoic acid for $C_{11}H_{14}O_3$) might also contribute to these ion signals. Several others are less likely to be found in the atmosphere since they are not directly used in formulations of volatile chemical products but rather as feedstocks for derivatives used in different industries. Some isomers such as vanillin and vanillylacetone are also used in food flavoring. Methyl paraben-related $C_8H_8O_3$ showed the highest concentration among these four ions ranging from 8 to 35 ppt across the sampling period. The remaining three had concentrations under 10 ppt throughout the sampling duration.

3.3.5 Select IVOCs related to coatings

The $C_{12}H_{24}O_3$ and $C_{16}H_{30}O_4$ ions were primarily attributed to texanol and 2,2,4-trimethyl-1,3-pentanediol diisobutyrate (TXIB) emissions that are widely used in coatings (Gkatzelis et al., 2021a). Even though estimated emissions of texanol ($1.9\text{-}2.5 \times 10^5$ kg yr^{-1}) are much higher than TXIB (2500 kg yr^{-1}; FIVE-VCP), and, texanol production on a national scale (45-110 Gg) considerably exceeds TXIB (22-44 Gg) (U.S. Environmental Protection Agency, Chemical Data Reporting, 2016), the concentrations of both these species had a similar range (5-30 ppt) with enhancements in TXIB concentrations above the 5th percentile background being comparable to texanol on average (Table 1). Given reduced photochemistry, this may suggest differences in outdoor vs indoor application, some geographical variability in their use and/or larger diversity in TXIB sources than texanol in this particular urban area.

3.3.6 Phthalates and Fatty-acid methyl esters (FAMEs)

Phthalates have received considerable attention in indoor environments but their concentrations in ambient air are relatively less constrained. In this study, the ion intensities of $C_{10}H_{10}O_4$ and $C_{12}H_{14}O_4$ include dimethyl phthalate (DMP) and diethyl phthalate (DEP), respectively, two commonly used phthalates in various consumer products. $C_{10}H_{10}O_4$ and $C_{12}H_{14}O_4$ had similar ion abundances across the 10-day sampling period. After accounting for differences in instrument response, $C_{10}H_{10}O_4$ concentrations were found to be smaller than $C_{12}H_{14}O_4$ throughout the campaign which aligns with DEP emission estimates being greater than DMP in NYC. The ambient concentrations of the two ions ranged between 5-30 ppt and often synchronously peaked between midnight and early morning hours (12-6 AM) while the lowest daily concentrations were observed during afternoons. These concentration trends indicated that unlike compounds associated with personal care products, phthalate concentrations were less influenced by outdoor human activities.

664   FAMEs are also an important class of compounds used in various consumer products. We
665   identified $C_9H_{18}O_2$ (e.g. methyl octanoate) and $C_{11}H_{22}O_2$ (e.g. methyl decanoate) ions via
666   CI-ToF that varied similarly in their abundances across the campaign period. $C_9H_{18}O_2$
667   concentrations ranged from 50 ppt to 200 ppt and showed slightly higher ion abundances
668   than $C_{11}H_{22}O_2$ even though the annual production of methyl octanoate for use in
669   consumer/commercial products (0.5-9 Gg) is considerably lower than methyl decanoate
670   (4.5-22 Gg) (U.S. Environmental Protection Agency, Chemical Data Reporting, 2016).
671   This suggested that isomers such as heptyl acetate and propyl hexanoate, which are used
672   in perfumes and food flavoring, may have also contributed to $C_9H_{18}O_2$ signal. Emissions
673   of pentyl butyrate, which has uses such as an additive in cigarettes are also possible. The
674   highest abundances in both $C_9H_{18}O_2$ and $C_{11}H_{22}O_2$ corresponded to wind currents from
675   Manhattan as well as the Bronx, which infers comparable emission rates within New
676   York City.

677

678   **3.4 Other observed ions of interest**

679   Of the total ions measured, a subset of isomers covering diverse chemical functionalities
680   were included for calibration while others were not calibrated or presented challenges
681   associated with their physiochemical properties that caused transmission issues during
682   LCS calibration. Hence, we will discuss trends in such ions in this subsection in terms of
683   their measured ion abundances (Table S3, figure S9). These include ions with likely
684   contributions from ethanolamines, organic acids, large alkyl methyl esters and some
685   oxygenated terpenoid compounds that are used in a wide range of volatile chemical
686   products.

687

688   Anthropogenic sources are major contributors of oxygenated terpenoid compounds (i.e.
689   oxy-terpenoids) in many urban areas, especially during wintertime. Among relevant ions
690   observed, $C_{10}H_{16}O$ (e.g. camphor), $C_{10}H_{18}O$ (e.g. linalool), $C_{10}H_{20}O$ (calibrated with
691   menthol) and $C_7H_{10}O$ (e.g. norcamphor) were the most prevalent in terms of measured
692   abundances. A number of isomers that are similarly used in various consumer products
693   likely contributed to their signal intensities. It is interesting to note that $C_{10}H_{16}O$
694   exhibited higher ion abundance than $C_{10}H_{18}O$ despite comparable estimated emissions of
695   camphor and linalool ($\sim 10^3$ kg yr^{-1}; VCPy) in NYC. This could be due to differences in
696   CI-ToF response factors, the magnitude of relative isomer contributions, seasonal trends
697   in the use of chemical species, or uncertainties in fragrance speciation within emissions
698   inventories. The peaks in abundances of all oxy-terpenoids were observed synchronously
699   in the morning hours between 8-10 AM and in the evening between 6-8 PM, consistent
700   with major commuting periods, especially when wind currents blew in from over

701   Manhattan from the south and south-east where the outdoor activity peaks during
702   morning and evening commute hours.

703

704   We detected C_2H_7NO, $C_4H_{11}NO_2$ and $C_6H_{15}NO_3$ ions at the site, representing
705   ethanolamine, diethanolamine, and triethanolamine, respectively. Of these, $C_4H_{11}NO_2$
706   and $C_6H_{15}NO_3$ followed trends of other VCPs-related compounds. $C_4H_{11}NO_2$ showed the
707   highest ion abundance throughout the campaign with the exception of a 24-hour period
708   between 26/1 and 27/1 when C_2H_7NO abundances increased dramatically. This peak in
709   C_2H_7NO was potentially caused by biomass burning since ions pertinent to 2-
710   methylfuran, methyl isocyanate, nitromethane and 2,5 dimethylfuran also peaked
711   simultaneously during this period. $C_4H_{11}NO_2$ showed much greater variations with wind
712   patterns, more similar to other VCPs, and peaks were noted in early morning hours
713   between 6-9 AM and during early evening hours around 6 PM. $C_6H_{15}NO_3$ showed lower
714   signal relative to C_2H_7NO and $C_4H_{11}NO_2$ which could be attributed to its smaller annual
715   production for use in consumer/commercial products (45-113 Gg), variations in CI-ToF
716   response factors and/or lower volatility that could decrease emission timescales and cause
717   it to partition to available surfaces indoors.

718

719   Several other major ions included $C_7H_{14}O_2$, $C_8H_{16}O_2$, $C_{12}H_{24}O_2$, $C_{16}H_{32}O_2$ and $C_{18}H_{34}O_2$
720   that were difficult to attribute to individual chemical species because of prevalence of
721   several possible isomers. These isomers were most probably esters and carboxylic acids
722   that are used in many consumer, commercial, and industrial applications. The esters
723   could have contributed more in some cases given their higher volatility, and also because
724   some carboxylic acids are used as feedstocks to produce esters. We briefly discuss these
725   ions here to guide future measurements.

726

727    $C_7H_{14}O_2$ was the most abundant ion in this group likely due to contributions from amyl
728   acetate, isoamyl acetate, and butyl propionate that are used as solvents,
729   fragrances/flavorings, and in other commercial/industrial applications, with possible
730   contributions from heptanoic acid. $C_8H_{16}O_2$ was the next most prominent and likely
731   related to octanoic acid, hexyl acetate, pentyl propanoate and butyl butyrate. $C_8H_{16}O_2$
732   emissions (~5×10^3 kg yr^{-1}) were predominantly (90%) estimated to be hexyl acetate by
733   the VCPy model. In comparison, amyl acetate (i.e. $C_7H_{14}O_2$) is estimated in much smaller
734   amounts across the two inventories (~5-500 kg yr^{-1}). Yet, the higher abundance of
735    $C_7H_{14}O_2$ suggested major contributions from other isomers and/or variations in CI-ToF
736   sensitivity. By comparison, we calibrated $C_8H_{16}O_2$ using octanoic acid given its
737   widespread use in various personal care and cosmetic products. This gave $C_8H_{16}O_2$

738   concentrations ranging from 50 to 300 ppt across the measurement period, but
739   considerable variation is possible with ester contributions to the ions' mass response
740   factors. Among other ions, the abundance of $C_{12}H_{24}O_2$ was comparable to $C_8H_{16}O_2$. The
741   larger ions, $C_{16}H_{32}O_2$ and $C_{18}H_{34}O_2$ showed very small (<10 ions s^{-1}) abundances
742   throughout the campaign. Interestingly, the low ion abundances occurred despite the
743   VCPy model's sizable emission estimates of alkyl methyl esters (C_{16}-C_{18}) on the order of
744   10^5 kg yr^{-1} in NYC, which is similar to more volatile esters such as methyl or ethyl
745   acetates. This highlights the importance of further research on these semi-volatile organic
746   compounds across seasons to examine if they have lower emissions or could have
747   partitioned to the particle phase in the atmosphere during the winter.

748

749   **3.5 Assessment of ambient concentrations relative to current emissions inventories**

750   In our analysis, high emission estimates did not always translate to high average ambient
751   concentrations and vice versa (Figures 7, S10), which warrants further examination of
752   ions (and contributing isomers) that were either highly abundant, differed significantly
753   from expected based on emissions inventories, or had limited prior measurements.
754   Though ambient concentrations of a chemical species may not always directly reflect the
755   magnitude of its primary emissions due to atmospheric processes, relative concentrations
756   are frequently used in studies to evaluate the relative magnitude of emissions of various
757   compounds (Gkatzelis et al., 2021a; Mcdonald et al., 2018).

758

759   Figures 7a-b shows the prevalence of such ions during the sampling period relative to
760   their estimated annual emissions against two different regionally-resolved inventories
761   specifically for NYC. The annual emissions were calculated as the sum of the annual
762   emissions of all isomers reported in inventories that contributed to each ion formula. Both
763   axes in figures 7a-b are ratioed to C_3H_6O (predominantly acetone) since it was among the
764   most abundant ions measured in this study and its primary isomer, acetone, has extensive,
765   diverse uses in various products and materials with the majority of anthropogenic
766   emissions coming from VCP-related sources. Still, we acknowledge that acetone, like
767   many oxygenated compounds, could see contributions from oxidation processes.
768   However, such secondary production would be at its minimum during this January study
769   period, and, the short timescales of emitted compounds' transport within the urban
770   footprint reduces (Figure S2) its potential influence in this analysis. Furthermore, to
771   account for any regional background influence in the calculation of emission ratios for
772   inventory comparisons, we have subtracted the estimated ambient background using the
773   5th percentile concentration value to focus on enhancements in the urban area during the
774   study, similar to prior work.

775

776 We also note that choosing an ideal denominator species in the middle of a complex,
777 dense urban environment with a wide array of spatiotemporally-dynamic sources is
778 highly challenging. Given the varying correlation coefficients between compounds
779 (Figure 6), Table 1 and Figure 7 are presented using geometric mean ratios of
780 concentration enhancements above the observed ambient background (i.e. 5th percentile).
781 This enables comparisons across all measured compounds, though a comparison of
782 concentration ratios versus slopes from least-squares regressions generally yielded
783 comparable results for acetone for well-correlated species (Figure S11). We note that this
784 comparison is done with data from January in a very densely populated area and acetone
785 concentrations will have seasonal variations from biogenic and secondary sources that
786 should be considered in future comparisons between seasons/sites. During this 10-day
787 period, the benzene-to-acetone ratio was close to that predicted by the VCPy inventory,
788 albeit with slightly greater than expected (i.e. 2:1) inferring additional benzene
789 anthropogenic or biomass burning related emissions than in the inventory (see Section 2),
790 but supports that acetone is not overestimated in the inventory when compared to a more
791 commonly-used anthropogenic tracer (i.e. benzene).

792

793 As common markers of anthropogenic activities, the observed ions were also compared
794 against CO and benzene, but, acetone and benzyl alcohol had a greater number of strong
795 correlations (0.9 < r < 1) in this densely populated area (Figure 6, Tables 1, S5).
796 Wherever appropriate, the following discussion in this subsection also draws upon
797 correlations with other ions that may inform source subtypes or emission pathways
798 (Figures S12-S15), with more detailed discussion available in the supplemental
799 information (SI). There was some variation in the number of speciated compounds
800 included in each inventory and, a subset of calibrated ions in this study were not available
801 in one of the emissions inventories. The compounds not speciated in VCPy are presented
802 in Figure 7c with mean concentrations relative to acetone.

803

804 Of the 58 calibrated ions, emissions of one or more isomers were reported for 38 ions in
805 VCPy and 32 ions in FIVE-VCP inventories. The ambient concentration ratios of roughly
806 half of these numbers agreed within 1 order of magnitude (i.e. 1:10, 10:1) with emissions
807 reported in both inventories (Figure 7a-b). Within this sub-fraction, concentrations of
808 50% of ions nearly matched with estimates, though with some variability between
809 inventories. In the case of VCPy (Figure 7a), some of the most accurately estimated ions
810 represented glycol and glycol ether compound categories, such as dipropylene- and
811 triethylene- glycols, 2-butoxyethanol, 2-methoxyethanol (with propylene glycol), and
812 phenoxyethanol, as well as D5, pentanedioic acid dimethyl ester, methyl pyrrolidone,

813   benzyl alcohol, monoterpenes and diethyl phthalate. Several other ions also representing
814   glycols and glycol ethers fell within the 1:10 range (Figure S16), but not ethylene glycol
815   (see discussion below).

816
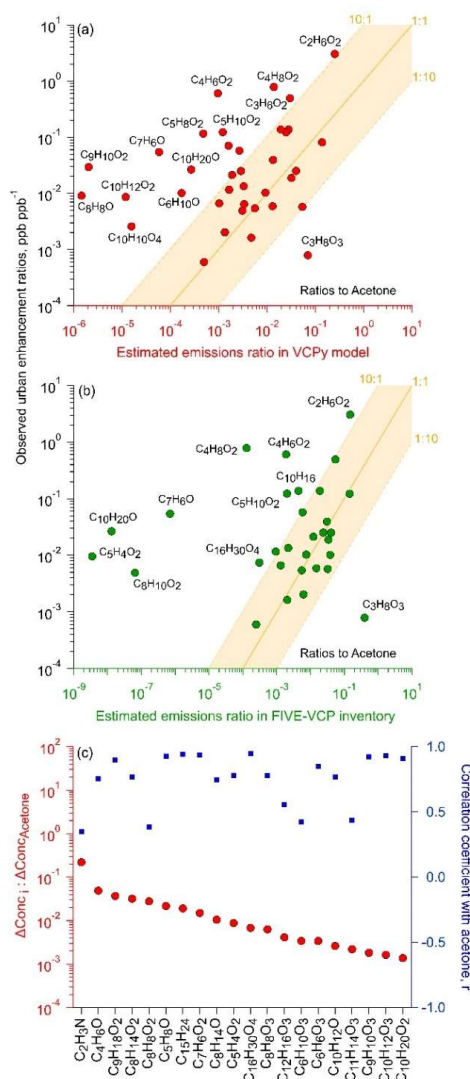
Figure 7. Comparison of ambient observations to emission inventories. Urban concentration enhancement ratios against acetone (calculated via background-subtracted geometric means) compared to estimated emission ratios using the (a) VCPy model and (b) FIVE-VCP inventory (shown for compounds with explicit estimates in each inventory, see Table 1). (c) Concentration enhancement ratios against acetone (and correlation coefficients) for calibrated ions where emissions data was not available in VCPy (panel a). Note: Examples of isomers contributing to ions in (a) and (b) are listed in Tables 1 and S4.

824   The ions in closest agreement with FIVE-VCP estimates shown in Figure 7b represented
825   benzyl alcohol, methyl pyrrolidone, MEK, D5 and a smaller number of glycol ethers that
826   included ethylene glycol hexyl ether, and, dipropylene- and diethylene- glycols. Other
827   ions within the tolerance bound included methyl- and butyl-acetates, 2-hexanone,
828   cyclohexanone and pentanedioic acid dimethyl ester. It is notable that ambient
829   measurements of glycols and glycol ethers made up approximately half of the total ions
830   that broadly agreed with emission estimates in both emissions inventories. Additionally,
831   the accuracy of benzyl alcohol estimates is also useful since ~45% of all mass calibrated
832   ions and ~35% of the total observed ions in this study correlated strongly ($0.9 < r < 1.0$)
833   with C_7H_8O (i.e. benzyl alcohol; Figures 6, S17-18), which may help in constraining
834   emissions in future studies.

835

836   The observed ambient ratios of the remaining ~50% ions deviated considerably from
837   those in emissions inventory estimates. The majority of these ions had greater
838   concentration ratios in Figure 7a-b, which suggests that their emissions were higher than
839   that expected based on emissions inventories. Among glycols in particular, ethylene
840   glycol was abundant with mean ambient concentration ratios slightly over 10 times the
841   inventory-based value. This result could be influenced by seasonal variations in use, such
842   as wintertime use as a de-icer for surfaces (or aircraft) or the particularly elevated
843   concentrations (25-35 ppb) during the first 4 days of the measurement period (Figure 5)
844   compared to the timeseries of other VOCs (Figure 4). Among glycol ethers, the $C_8H_{10}O_2$
845   ion representing phenoxyethanol differed considerably between the two inventories,
846   ranging from near expected in VCPy to a much higher ambient abundance relative to
847   FIVE-VCP (Figure S16). This was likely due to estimated phenoxyethanol emissions
848   being 10^5 times higher in VCPy than in FIVE-VCP. However, 1,4-dimethoxybenzene
849   might have also contributed to $C_8H_{10}O_2$ ion signal given its widespread use in personal
850   care products but needs inclusion in emissions inventories. Similarly, monoterpenes
851   during this study slightly exceeded the 10:1 value based on FIVE-VCP estimates (Figure
852   7), which was influenced by significantly different limonene emissions between the two
853   inventories (60206 kg yr^{-1}; VCPy vs 17107 kg yr^{-1}; FIVE-VCP) that constituted over
854   90% of the reported monoterpene emissions. D4-siloxane deviated in the other direction
855   going from near expected in FIVE-VCP to considerably above the 10:1 bound in VCPy
856   comparisons, which was likely due to a factor of 8 difference in its reported emissions
857   between the two inventories. The cyclohexanone-related $C_6H_{10}O$ concentration ratio was
858   somewhat lower than expected based on FIVE-VCP estimates though within the lower
859   tolerance bound, but substantially exceeded VCPy estimates (Figure S16) given the
860   ~280-fold difference in cyclohexanone emissions between the two inventories.

861

862   Some ions deviated even more substantially in ambient concentration ratios relative to
863   inventory-based expectations (Figure 7a). The prominent ions in this group represented
864   esters, e.g. $C_9H_{10}O_2$ (e.g. benzyl acetate), $C_4H_6O_2$ (e.g. methyl acrylate), $C_5H_8O_2$ (e.g.
865   MMA), $C_5H_{10}O_2$ (e.g. isopropyl acetate) and $C_4H_8O_2$ (e.g. ethyl acetate). All these
866   compounds (except MMA) are found in solvents, fragrances, food flavorings, and
867   naturally in some food (e.g. fruits). Some fraction of their discrepancies may be attributed
868   to uncertain fragrances source categories in emissions inventories which contributes, in
869   part, to their higher than expected concentrations in our analysis. Hence, further work is
870   needed to more comprehensively speciate and constrain fragrance-related emissions.
871   Other possibilities for these differences include missing sources that need to be accounted
872   for in estimating total emissions for each ion. For example, diacetyl is also a likely
873   isomer of $C_4H_6O_2$ that is currently excluded from emissions inventories. MMA
874   concentrations at 100's of parts per trillion (Figure 5) is an interesting case due to its
875   minimal use in consumer products, and, besides contributions from other isomers to
876    $C_5H_8O_2$ ion, may indicate ambient observations of PMMA offgassing/degradation under
877   ambient conditions. Similarly, higher than expected $C_{10}H_{10}O_4$ (e.g. dimethyl phthalate)
878   concentrations could be contributed to by materials-related off-gassing and emissions
879   from personal care products.

880

881   Ions related to benzaldehyde and menthol also exhibited higher than expected
882   concentrations in both inventory assessments. $C_{10}H_{20}O$ (e.g. menthol) showed strong
883   correlations ($r > 0.95$) with 14 other ions that spanned several compound classes
884   including glycol ethers, carbonyls, esters and alcohol. This may be also contributed to by
885   fragrance-related sources, or other isomers in the case of menthol. $C_9H_{10}O_2$ (e.g. benzyl
886   acetate), $C_{10}H_{12}O_2$ (e.g. eugenol) and $C_6H_{10}O$ (e.g. cyclohexanone) ions also showed high
887   concentrations in VCPy inventory comparisons while $C_5H_4O_2$ (e.g. furfural) exceeded
888   expected concentrations based on FIVE-VCP estimates. Furfural could also be
889   contributed by indoor emissions from wood-based materials (Sheu et al., 2021) though
890   such a source will be lower in NYC than observed elsewhere given major differences in
891   Manhattan building construction materials. Some of these isomers, e.g. eugenol,
892   raspberry ketone and furfural are also used in food flavorings, which remains largely
893   unexplored as a potential source of emissions.

894

895   The glycerol-related $C_3H_8O_3$ ion presents a very interesting case among the few ions that
896   exhibited considerably lower concentrations than expected. Its annual estimated
897   emissions are comparable to prominent carbonyls and esters with slight differences
898   between the VCPy and FIVE-VCP inventories ($\sim10^5$ kg yr^{-1} vs. $\sim10^6$ kg yr^{-1}). However, it
899   is uncertain whether its low mean concentration during the sampling period (Table 1) was

900   influenced by seasonal variations in ambient gas-to-particle partitioning and/or in
901   emissions pathways (e.g. reduced evaporation or indoor-to-outdoor transport). Thus,
902   further research would be valuable to evaluate atmospheric levels of glycerol including
903   during summertime conditions when evaporative emissions from personal care products
904   and indoor-to-outdoor transport are enhanced relative to January. The same factors may
905   have also driven the somewhat lower concentrations of texanol relative to inventory-
906   based predictions (Figures 7a-b, S16), though its concentrations are similar to
907   summertime observations in NYC (Stockwell et al., 2021).

908

909   Among ions without any emissions estimates, $C_8H_8O_2$ (e.g. methyl benzoate), $C_9H_{18}O_2$
910   (e.g. heptyl acetate) and $C_7H_6O_2$ (e.g. benzoic acid) had some of the highest
911   concentration ratios to acetone (Figure 7c), and may warrant inclusion in emission
912   inventories, potentially as part of "fragrances" or other uncertain source types.
913   Observations of sesquiterpenes were 7% of acetone concentrations on average (Table 1).
914   The mean sesquiterpenes to monoterpenes ratio was ~0.5 during the measurement period
915   though sensitive to instrument calibration, emphasizing sizable contributions from the
916   highly-reactive sesquiterpenes to urban air. Ions including C_4H_6O (e.g. MVK), $C_8H_{14}O_2$
917   (e.g. cyclohexyl acetate), C_5H_8O (e.g. cyclopentanone) and $C_8H_{14}O$ (e.g. 6-methyl-5-
918   hepten-2-one, a skin oil oxidation product) were not estimated in the inventory, but
919   showed very strong correlations ($0.9 < r < 1.0$) with the acetone-related C_3H_6O ion.

920

921   **4. Conclusions and future work**

922   A Vocus CI-ToF using low-pressure NH_4^+ as the reagent ion enabled measurements of a
923   wide range of oxygenated species in New York City whose enhancements were primarily
924   attributed to anthropogenic sources given the wintertime conditions. Our results highlight
925   the diversity of oxygenated compounds in urban air, including VCP-related compounds
926   that extend considerably beyond the highly volatile, functionalized species found in
927   oxygenated solvents. The measured ions had contributions from VOCs to I/SVOCs
928   including acetates, glycols, glycol ethers, alcohols, acrylates and other functional groups.
929   The atmospheric concentrations of these species varied over a large range but reached up
930   to hundreds of ppt and into ppb-levels in several cases, which were comparable to the
931   prevalence of known prominent OVOCs such as acetone, MEK and MVK. While
932   emissions inventories predicted the relative abundance of many species in the atmosphere
933   with relative accuracy (e.g. glycols and glycol ethers), several others deviated
934   significantly (e.g. esters). This informs new avenues for investigation of the emissions or
935   atmospheric dynamics of these species indoors or outdoors, and possible additional
936   compounds and source contributions for inclusion in emissions inventories. Given the
937   high ambient prevalence of some species, further research is also warranted to further

938 enhance chemical speciation in inventories (and measurements) that will constrain
939 potential contributions to SOA and ozone formation under varying environmental
940 conditions. Future summertime studies (e.g. AEROMMA, GOTHAAM) will also provide
941 valuable opportunities to compare seasonal abundances of observed species and to study
942 different seasonally-dependent emission pathways.

943

Author Contributions

945 D.R.G., J.E.M. (SBU), and J.E.K. conceived the study, and J.E.K. performed the ambient
946 Vocus CI-ToF measurements with support from R.T.C. P.K. led data analysis and writing
947 with support from J.E.K and D.R.G., and contributions/review from other co-authors.
948 P.K., J.E.M. (Yale) and J.W. prepared calibration mixes. J.E.M. (Yale), J.W. and J.E.K
949 performed in-lab calibrations. T.H.M. collected EI-MS samples and conducted related
950 analysis, along with J.W. and J.E.M. (Yale). K.M.S and H.O.T.P. developed the VCPy
951 model and K.M.S. performed VCPy calculations for this work. B.M. provided the FIVE-
952 VCP emissions inventory data used in this study. F.M. and F.L.H. developed and tested
953 the Vocus CI-ToF instrument for this study. C.C. and J.E.M. (SBU) performed PTR-ToF
954 measurements used for instrument cross-validation in this study. R.C. provided carbon
955 monoxide data and R.T.C. helped setting up the measurement site.

956

Competing interests

958 Jordan E. Krechmer is employed by Aerodyne Research, Inc., which commercializes the
959 Vocus CI-ToF instrument for geoscience research and Felipe Lopez-Hilfiker is an
960 employee of Tofwerk, AG, which manufactures and sells the Vocus CI-ToF instrument
961 used in this study.

962

Acknowledgements

964 We thank the Northeast States for Coordinated Air Use Management (NESCAUM) for
965 funding this research through a contract with the New York State Energy and
966 Development Authority (NYSERDA) (Agreement No. 101132) as part of the LISTOS
967 project. Any opinions expressed in this article do not necessarily reflect those of
968 NYSERDA or the State of New York. We also would like to acknowledge financial
969 support from U.S. NSF (CBET-2011362 and AGS-1764126), and Columbia University.
970 We thank the City University of New York for facilitating sampling at their Advanced
971 Science Research Center. The views expressed in this article are those of the authors and
972 do not necessarily represent the views or policies of the U.S. Environmental Protection
973 Agency.

974

975 **References**

976 U.S. Environmental Protection Agency, Chemical Data Reporting 2016, [online]
977 Available from: https://www.epa.gov/chemical-data-reporting/access-cdr-data, 2016.

978 Asaf, D., Tas, E., Pedersen, D., Peleg, M. and Luria, M.: Long-Term Measurements of
979 NO3 Radical at a Semiarid Urban Site: 2. Seasonal Trends and Loss Mechanisms,
980 Environ. Sci. Technol. , 44, 5901–5907, doi:10.1021/es100967z, 2010.

981 Aschmann, S. M., Martin, P., Tuazon, E. C., Arey, J. and Atkinson, R.: Kinetic and
982 product studies of the reactions of selected glycol ethers with OH radicals, Environ. Sci.
983 Technol., 35(20), 4080–4088,
984 doi:10.1021/ES010831K/SUPPL_FILE/ES010831K_S.PDF, 2001.

985 Bennet, F., Hart-Smith, G., Gruendling, T., Davis, T. P., Barker, P. J. and Barner-
986 Kowollik, C.: Degradation of poly(methyl methacrylate) model compounds under
987 extreme environmental conditions, Macromol. Chem. Phys., 211(13), 1083–1097, 2010.

988 Bi, C., Liang, Y. and Xu, Y.: Fate and Transport of Phthalates in Indoor Environments
989 and the Influence of Temperature: A Case Study in a Test House, Environ. Sci. Technol.,
990 49(16), 9674–9681, doi:10.1021/acs.est.5b02787, 2015.

991 Bi, C., Krechmer, J. E., Frazier, G. O., Xu, W., Lambe, A. T., Claflin, M. S., Lerner, B.
992 M., Jayne, J. T., Worsnop, D. R., Canagaratna, M. R. and Isaacman-Vanwertz, G.:
993 Quantification of isomer-resolved iodide chemical ionization mass spectrometry
994 sensitivity and uncertainty using a voltage-scanning approach, Atmos. Meas. Tech.,
995 14(10), 6835–6850, doi:10.5194/AMT-14-6835-2021, 2021.

996 Bornehag, C. G., Lundgren, B., Weschler, C. J., Sigsgaard, T., Hagerhed-Engman, L. and
997 Sundell, J.: Phthalates in indoor dust and their association with building characteristics,
998 Environ. Health Perspect., 113(10), 1399–1404, doi:10.1289/ehp.7809, 2005.

999 Canaval, E., Hyttinen, N., Schmidbauer, B., Fischer, L. and Hansel, A.: NH4+
1000 association and proton transfer reactions with a series of organic molecules, Front.
1001 Chem., 7(APR), 191, doi:10.3389/FCHEM.2019.00191/BIBTEX, 2019.

1002 Cao, H., Li, X., He, M. and Zhao, X. S.: Computational study on the mechanism and
1003 kinetics of NO3-initiated atmosphere oxidation of vinyl acetate, Comput. Theor. Chem.,
1004 1144, 18–25, doi:10.1016/J.COMPTC.2018.09.012, 2018.

1005 Charan, S. M., Buenconsejo, R. S. and Seinfeld, J. H.: Secondary organic aerosol yields
1006 from the oxidation of benzyl alcohol, Atmos. Chem. Phys., 20(21), 13167–13190,
1007 doi:10.5194/ACP-20-13167-2020, 2020.

1008 Choi, H., Schmidbauer, N., Sundell, J., Hasselgren, M., Spengler, J. and Bornehag, C. G.:
1009 Common household chemicals and the allergy risks in pre-school age children, PLoS
1010 One, 5(10), doi:10.1371/journal.pone.0013423, 2010a.

1011 Choi, H., Schmidbauer, N., Spengler, J. and Bornehag, C. G.: Sources of propylene
1012 glycol and glycol ethers in air at home, Int. J. Environ. Res. Public Health, 7(12), 4213–

4237, doi:10.3390/ijerph7124213, 2010b.

Coggon, M. M., McDonald, B. C., Vlasenko, A., Veres, P. R., Bernard, F., Koss, A. R., Yuan, B., Gilman, J. B., Peischl, J., Aikin, K. C., Durant, J., Warneke, C., Li, S. M. and De Gouw, J. A.: Diurnal Variability and Emission Pattern of Decamethylcyclopentasiloxane (D5) from the Application of Personal Care Products in Two North American Cities, Environ. Sci. Technol., 52(10), 5610–5618, doi:10.1021/acs.est.8b00506, 2018.

Coggon, M. M., Gkatzelis, G. I., McDonald, B. C., Gilman, J. B., Schwantes, R. H., Abuhassan, N., Aikin, K. C., Arendd, M. F., Berkoff, T. A., Brown, S. S., Campos, T. L., Dickerson, R. R., Gronoff, G., Hurley, J. F., Isaacman-Vanwertz, G., Koss, A. R., Li, M., McKeen, S. A., Moshary, F., Peischl, J., Pospisilova, V., Ren, X., Wilson, A., Wu, Y., Trainer, M. and Warneke, C.: Volatile chemical product emissions enhance ozone and modulate urban chemistry, Proc. Natl. Acad. Sci. U. S. A., 118(32), doi:10.1073/PNAS.2026653118/SUPPL_FILE/PNAS.2026653118.SAPP.PDF, 2021.

Coggona, M. M., Gkatzelis, G. I., McDonald, B. C., Gilman, J. B., Schwantes, R. H., Abuhassan, N., Aikin, K. C., Arendd, M. F., Berkoff, T. A., Brown, S. S., Campos, T. L., Dickerson, R. R., Gronoff, G., Hurley, J. F., Isaacman-Vanwertz, G., Koss, A. R., Li, M., McKeen, S. A., Moshary, F., Peischl, J., Pospisilova, V., Ren, X., Wilson, A., Wu, Y., Trainer, M. and Warneke, C.: Volatile chemical product emissions enhance ozone and modulate urban chemistry, Proc. Natl. Acad. Sci. U. S. A., 118(32), doi:10.1073/PNAS.2026653118/SUPPL_FILE/PNAS.2026653118.SAPP.PDF, 2021.

Council of the European Union: EU Directive 1999/13/EC: Reducing the emissions of volatile organic compounds (VOCs). [online] Available from: eur-lex.europa.eu/legal-content/EN/TXT/?uri=celex:31999L0013, 1999.

Destaillats, H., Lunden, M. M., Singer, B. C., Coleman, B. K., Hodgson, A. T., Weschler, C. J. and Nazaroff, W. W.: Indoor Secondary Pollutants from Household Product Emissions in the Presence of Ozone: A Bench-Scale Chamber Study, Environ. Sci. Technol., 40, 4421–4428, doi:10.1021/ES052198Z, 2006.

Even, M., Girard, M., Rich, A., Hutzler, C. and Luch, A.: Emissions of VOCs From Polymer-Based Consumer Products: From Emission Data of Real Samples to the Assessment of Inhalation Exposure, Front. Public Heal., 7, 202, doi:10.3389/fpubh.2019.00202, 2019.

Even, M., Hutzler, C., Wilke, O. and Luch, A.: Emissions of volatile organic compounds from polymer-based consumer products: Comparison of three emission chamber sizes, Indoor Air, 30(1), 40–48, doi:10.1111/ina.12605, 2020.

Franco, B., Blumenstock, T., Cho, C., Clarisse, L., Clerbaux, C., Coheur, P. F., De Mazière, M., De Smedt, I., Dorn, H. P., Emmerichs, T., Fuchs, H., Gkatzelis, G., Griffith, D. W. T., Gromov, S., Hannigan, J. W., Hase, F., Hohaus, T., Jones, N., Kerkweg, A., Kiendler-Scharr, A., Lutsch, E., Mahieu, E., Novelli, A., Ortega, I., Paton-Walsh, C., Pommier, M., Pozzer, A., Reimer, D., Rosanka, S., Sander, R., Schneider, M., Strong, K., Tillmann, R., Van Roozendael, M., Vereecken, L., Vigouroux, C., Wahner, A. and Taraborrelli, D.: Ubiquitous atmospheric production of organic acids mediated by cloud

droplets, Nat. 2021 5937858, 593(7858), 233–237, doi:10.1038/s41586-021-03462-x, 2021.

Gkatzelis, G. I., Coggon, M. M., McDonald, B. C., Peischl, J., Aikin, K. C., Gilman, J. B., Trainer, M. and Warneke, C.: Identifying Volatile Chemical Product Tracer Compounds in U.S. Cities, Environ. Sci. Technol., 55(1), 188–199, doi:10.1021/ACS.EST.0C05467/SUPPL_FILE/ES0C05467_SI_001.PDF, 2021a.

Gkatzelis, G. I., Coggon, M. M., McDonald, B. C., Peischl, J., Gilman, J. B., Aikin, K. C., Robinson, M. A., Canonaco, F., Prevot, A. S. H., Trainer, M. and Warneke, C.: Observations Confirm that Volatile Chemical Products Are a Major Source of Petrochemical Emissions in U.S. Cities, Environ. Sci. Technol., 55(8), 4332–4343, doi:10.1021/ACS.EST.0C05471/SUPPL_FILE/ES0C05471_SI_001.PDF, 2021b.

de Gouw, J. A., Gilman, J. B., Kim, S. W., Lerner, B. M., Isaacman-VanWertz, G., McDonald, B. C., Warneke, C., Kuster, W. C., Lefer, B. L., Griffith, S. M., Dusanter, S., Stevens, P. S. and Stutz, J.: Chemistry of Volatile Organic Compounds in the Los Angeles basin: Nighttime Removal of Alkenes and Determination of Emission Ratios, J. Geophys. Res. Atmos., 122(21), 11,843-11,861, doi:10.1002/2017JD027459, 2017.

Harb, P., Locoge, N. and Thevenet, F.: Treatment of household product emissions in indoor air: Real scale assessment of the removal processes, Chem. Eng. J., 380, 122525, doi:10.1016/j.cej.2019.122525, 2020.

Heald, C. L. and Kroll, J. H.: The fuel of atmospheric chemistry: Toward a complete description of reactive organic carbon, Sci. Adv., 6(6), eaay8967, doi:10.1126/sciadv.aay8967, 2020.

Henze, D. K., Seinfeld, J. H., Ng, N. L., Kroll, J. H., Fu, T. M., Jacob, D. J. and Heald, C. L.: Global modeling of secondary organic aerosol formation from aromatic hydrocarbons: High- vs. low-yield pathways, Atmos. Chem. Phys., 8(9), 2405–2421, doi:10.5194/ACP-8-2405-2008, 2008.

Humes, M. B., Wang, M., Kim, S., Machesky, J. E., Gentner, D. R., Robinson, A. L., Donahue, N. M. and Presto, A. A.: Limited Secondary Organic Aerosol Production from Acyclic Oxygenated Volatile Chemical Products, Environ. Sci. Technol., 56(8), 4806–4815, doi:10.1021/acs.est.1c07354, 2022.

Karl, T., Striednig, M., Graus, M., Hammerle, A. and Wohlfahrt, G.: Urban flux measurements reveal a large pool of oxygenated volatile organic compound emissions, , 115(6), 1186–1191, doi:10.1073/pnas.1714715115, 2018.

Khare, P. and Gentner, D. R.: Considering the future of anthropogenic gas-phase organic compound emissions and the increasing influence of non-combustion sources on urban air quality, Atmos. Chem. Phys., 18(8), doi:10.5194/acp-18-5391-2018, 2018.

Khare, P., Machesky, J., Soto, R., He, M., Presto, A. A. and Gentner, D. R.: Asphalt-related emissions are a major missing nontraditional source of secondary organic aerosol precursors, Sci. Adv., 6(36), eabb9785, 2020.

Krechmer, J., Lopez-Hilfiker, F., Koss, A., Hutterli, M., Stoermer, C., Deming, B.,

Kimmel, J., Warneke, C., Holzinger, R., Jayne, J., Worsnop, D., Fuhrer, K., Gonin, M. and De Gouw, J.: Evaluation of a New Reagent-Ion Source and Focusing Ion− Molecule Reactor for Use in Proton-Transfer-Reaction Mass Spectrometry, , 90(20), 12011–12018, doi:10.1021/acs.analchem.8b02641, 2018.

Krechmer, J. E., Pagonis, D., Ziemann, P. J. and Jimenez, J. L.: Quantification of Gas-Wall Partitioning in Teflon Environmental Chambers Using Rapid Bursts of Low-Volatility Oxidized Species Generated in Situ, Environ. Sci. Technol., 50(11), 5757–5765, doi:10.1021/acs.est.6b00606, 2016.

Li, W., Li, L., Chen, C. li, Kacarab, M., Peng, W., Price, D., Xu, J. and Cocker, D. R.: Potential of select intermediate-volatility organic compounds and consumer products for secondary organic aerosol and ozone formation under relevant urban conditions, Atmos. Environ., 178, 109–117, doi:10.1016/J.ATMOSENV.2017.12.019, 2018.

Liang, Y., Caillot, O., Zhang, J., Zhu, J. and Xu, Y.: Large-scale chamber investigation and simulation of phthalate emissions from vinyl flooring, Build. Environ., 89, 141–149, doi:10.1016/j.buildenv.2015.02.022, 2015.

Mansouri, K., Grulke, C. M., Judson, R. S. and Williams, A. J.: OPERA models for predicting physicochemical properties and environmental fate endpoints, J. Cheminform., 10(1), 1–19, doi:10.1186/S13321-018-0263-1/FIGURES/1, 2018.

Markowicz, P. and Larsson, L.: Influence of relative humidity on VOC concentrations in indoor air, Environ. Sci. Pollut. Res., 22(8), 5772–5779, doi:10.1007/s11356-014-3678-x, 2015.

Masuck, I., Hutzler, C., Jann, O. and Luch, A.: Inhalation exposure of children to fragrances present in scented toys, Indoor Air, 21(6), 501–511, doi:10.1111/j.1600-0668.2011.00727.x, 2011.

Mcdonald, B. C., De Gouw, J. A., Gilman, J. B., Jathar, S. H., Akherati, A., Cappa, C. D., Jimenez, J. L., Lee-Taylor, J., Hayes, P. L., Mckeen, S. A., Cui, Y. Y., Kim, S.-W., Gentner, D. R., Isaacman-Vanwertz, G., Goldstein, A. H., Harley, R. A., Frost, G. J., Roberts, J. M., Ryerson, T. B. and Trainer, M.: Volatile chemical products emerging as largest petrochemical source of urban organic emissions, Science (80-.)., 359(6377), 760–764 [online] Available from: http://science.sciencemag.org/content/sci/359/6377/760.full.pdf (Accessed 25 February 2018), 2018.

McLachlan, M. S., Kierkegaard, A., Hansen, K. M., Van Egmond, R., Christensen, J. H. and Skjøth, C. A.: Concentrations and fate of decamethylcyclopentasiloxane (D5) in the atmosphere, Environ. Sci. Technol., 44(14), 5365–5370, doi:10.1021/es100411w, 2010.

Mellouki, A., Wallington, T. J. and Chen, J.: Atmospheric Chemistry of Oxygenated Volatile Organic Compounds: Impacts on Air Quality and Climate, Chem. Rev., 115(10), 3984–4014, doi:10.1021/CR500549N/ASSET/IMAGES/CR500549N.SOCIAL.JPEG_V03, 2015.

Noguchi, M. and Yamasaki, A.: Volatile and semivolatile organic compound emissions from polymers used in commercial products during thermal degradation, Heliyon, 6(3),

1136   e03314, doi:10.1016/j.heliyon.2020.e03314, 2020.

1137   Pagonis, D., Krechmer, J. E., De Gouw, J., Jimenez, J. L. and Ziemann, P. J.: Effects of
1138   gas–wall partitioning in Teflon tubing and instrumentation on time-resolved
1139   measurements of gas-phase organic compounds, Atmos. Meas. Tech, 10, 4687–4696,
1140   doi:10.5194/amt-10-4687-2017, 2017.

1141   Pennington, E. A., Seltzer, K. M., Murphy, B. N., Qin, M., Seinfeld, J. H. and Pye, H. O.
1142   T.: Modeling secondary organic aerosol formation from volatile chemical products,
1143   Atmos. Chem. Phys., 21(24), 18247–18261, doi:10.5194/ACP-21-18247-2021, 2021.

1144   Picquet-Varrault, B., Doussin, J. F., Durand-Jolibois, R., Pirali, O., Carlier, P. and
1145   Fittschen, C.: Kinetic and Mechanistic Study of the Atmospheric Oxidation by OH
1146   Radicals of Allyl Acetate, Environ. Sci. Technol., 36(19), 4081–4086,
1147   doi:10.1021/ES0200138, 2002.

1148   Pye, H. O. T., Ward-Caviness, C. K., Murphy, B. N., Appel, K. W. and Seltzer, K. M.:
1149   Secondary organic aerosol association with cardiorespiratory disease mortality in the
1150   United States, Nat. Commun., 12(1), doi:10.1038/S41467-021-27484-1, 2021.

1151   Qin, M., Murphy, B. N., Isaacs, K. K., McDonald, B. C., Lu, Q., McKeen, S. A., Koval,
1152   L., Robinson, A. L., Efstathiou, C., Allen, C. and Pye, H. O. T.: Criteria pollutant impacts
1153   of volatile chemical products informed by near-field modelling, Nat. Sustain. 2020 42,
1154   4(2), 129–137, doi:10.1038/s41893-020-00614-1, 2020.

1155   Ren, X., Brune, W. H., Mao, J., Mitchell, M. J., Lesher, R. L., Simpas, J. B., Metcalf, A.
1156   R., Schwab, J. J., Cai, C., Li, Y., Demerjian, K. L., Felton, H. D., Boynton, G., Adams,
1157   A., Perry, J., He, Y., Zhou, X. and Hou, J.: Behavior of OH and HO2 in the winter
1158   atmosphere in New York City, Atmos. Environ., 40(SUPPL. 2), 252–263,
1159   doi:10.1016/J.ATMOSENV.2005.11.073, 2006.

1160   Ren, Y., El Baramoussi, E. M., Daële, V. and Mellouki, A.: Atmospheric chemistry of
1161   ketones: Reaction of OH radicals with 2-methyl-3-pentanone, 3-methyl-2-pentanone and
1162   4-methyl-2-pentanone, Sci. Total Environ., 780,
1163   doi:10.1016/J.SCITOTENV.2021.146249, 2021.

1164   Schroder, J. C., Campuzano-Jost, P., Day, D. A., Shah, V., Larson, K., Sommers, J. M.,
1165   Sullivan, A. P., Campos, T., Reeves, J. M., Hills, A., Hornbrook, R. S., Blake, N. J.,
1166   Scheuer, E., Guo, H., Fibiger, D. L., McDuffie, E. E., Hayes, P. L., Weber, R. J., Dibb, J.
1167   E., Apel, E. C., Jaeglé, L., Brown, S. S., Thornton, J. A. and Jimenez, J. L.: Sources and
1168   Secondary Production of Organic Aerosols in the Northeastern United States during
1169   WINTER, J. Geophys. Res. Atmos., 123(14), 7771–7796, doi:10.1029/2018JD028475,
1170   2018.

1171   Schwarz, J., Makeš, O., Ondráček, J., Cusack, M., Talbot, N., Vodička, P., Kubelová, L.
1172   and Ždímal, V.: Single Usage of a Kitchen Degreaser Can Alter Indoor Aerosol
1173   Composition for Days, Environ. Sci. Technol., 51(11), 5907–5912,
1174   doi:10.1021/acs.est.6b06050, 2017.

1175   Seltzer, K. M., Pennington, E., Rao, V., Murphy, B. N., Strum, M., Isaacs, K. K., Pye, H.
1176   O. T. and Pye, H.: Reactive organic carbon emissions from volatile chemical products,

Atmos. Chem. Phys, 21, 5079–5100, doi:10.5194/acp-21-5079-2021, 2021.

Seltzer, K. M., Murphy, B. N., Pennington, E. A., Allen, C., Talgo, K. and Pye, H. O. T.: Volatile Chemical Product Enhancements to Criteria Pollutants in the United States, Environ. Sci. Technol., 56(11), 6905–6913, doi:10.1021/ACS.EST.1C04298/SUPPL_FILE/ES1C04298_SI_001.PDF, 2022.

Shah, R. U., Coggon, M. M., Gkatzelis, G. I., McDonald, B. C., Tasoglou, A., Huber, H., Gilman, J., Warneke, C., Robinson, A. L. and Presto, A. A.: Urban Oxidation Flow Reactor Measurements Reveal Significant Secondary Organic Aerosol Contributions from Volatile Emissions of Emerging Importance, Environ. Sci. Technol., 54(2), 714–725, doi:10.1021/acs.est.9b06531, 2020.

Sheu, R., Marcotte, A., Khare, P., Charan, S., Ditto, J. and Gentner, D. R.: Advances in offline approaches for speciated measurements of trace gas-phase organic compounds via an integrated sampling-to-analysis system, J. Chromatogr. A, 1575, 80–90, doi:https://doi.org/10.1016/j.chroma.2018.09.014, 2018.

Sheu, R., Stönner, C., Ditto, J. C., Klüpfel, T., Williams, J. and Gentner, D. R.: Human transport of thirdhand tobacco smoke: A prominent source of hazardous air pollutants into indoor nonsmoking environments, Sci. Adv., 6(10), eaay4109, doi:10.1126/sciadv.aay4109, 2020.

Sheu, R., Fortenberry, C. F., Walker, M. J., Eftekhari, A., Stönner, C., Bakker, A., Peccia, J., Williams, J., Morrison, G. C., Williams, B. J. and Gentner, D. R.: Evaluating Indoor Air Chemical Diversity, Indoor-to-Outdoor Emissions, and Surface Reservoirs Using High-Resolution Mass Spectrometry, Environ. Sci. Technol., 55(15), 10255–10267, doi:10.1021/ACS.EST.1C01337/SUPPL_FILE/ES1C01337_SI_001.PDF, 2021.

Shi, S., Cao, J., Zhang, Y. and Zhao, B.: Emissions of Phthalates from Indoor Flat Materials in Chinese Residences, Environ. Sci. Technol., 52(22), 13166–13173, doi:10.1021/acs.est.8b03580, 2018.

Singer, B. C., Destaillats, H., Hodgson, A. T. and Nazaroff, W. W.: Cleaning products and air fresheners: Emissions and resulting concentrations of glycol ethers and terpenoids, Indoor Air, 16(3), 179–191, doi:10.1111/j.1600-0668.2005.00414.x, 2006.

Stockwell, C. E., Coggon, M. M., I. Gkatzelis, G., Ortega, J., McDonald, B. C., Peischl, J., Aikin, K., Gilman, J. B., Trainer, M. and Warneke, C.: Volatile organic compound emissions from solvent-and water-borne coatings-compositional differences and tracer compound identifications, Atmos. Chem. Phys., 21(8), 6005–6022, doi:10.5194/ACP-21-6005-2021, 2021.

Venecek, M. A., Carter, W. P. L. and Kleeman, M. J.: Updating the SAPRC Maximum Incremental Reactivity (MIR) scale for the United States from 1988 to 2010, J. Air Waste Manag. Assoc., 68(12), 1301–1316, doi:10.1080/10962247.2018.1498410/SUPPL_FILE/UAWM_A_1498410_SM9019.DOCX, 2018.

Wang, C., Collins, D. B., Arata, C., Goldstein, A. H., Mattila, J. M., Farmer, D. K., Ampollini, L., DeCarlo, P. F., Novoselac, A., Vance, M. E., Nazaroff, W. W. and Abbatt,

1218   J. P. D.: Surface reservoirs dominate dynamic gas-surface partitioning of many indoor air
1219   constituents, Sci. Adv., 6(8), 8973,
1220   doi:10.1126/SCIADV.AAY8973/SUPPL_FILE/AAY8973_SM.PDF, 2020.

1221   Warneke, C., Schwantes, R., Veres, P., Rollins, A., Brewer, W. A., Mcdonald, B.,
1222   Brown, S., Frost, G., Fahey, D., Aikin, K., Mak, J., Holden, B., Giles, D., Tom, P. :,
1223   Tolnet, H., Sullivan, J., Valin, L., Szykman, J., Quinn, T., Bates, T. and Russell, L.:
1224   Atmospheric Emissions and Reactions Observed from Megacities to Marine Areas
1225   (AEROMMA 2023), [online] Available from: https://csl.noaa.gov/projects/aeromma/
1226   (Accessed 3 June 2022), n.d.

1227   Wensing, M., Uhde, E. and Salthammer, T.: Plastics additives in the indoor
1228   environment—flame retardants and plasticizers, Sci. Total Environ., 339(1), 19–40,
1229   doi:10.1016/j.scitotenv.2004.10.028, 2005.

1230   Weschler, C. J. and Nazaroff, W. W.: Semivolatile organic compounds in indoor
1231   environments, Atmos. Environ., 42(40), 9018–9040,
1232   doi:10.1016/j.atmosenv.2008.09.052, 2008.

1233   Westmore, J. B. and Alauddin, M. M.: Ammonia chemical ionization mass spectrometry,
1234   Mass Spectrom. Rev., 5(4), 381–465, doi:10.1002/MAS.1280050403, 1986.

1235   Zaytsev, A., Koss, A. R., Breitenlechner, M., Krechmer, J. E., Nihill, K. J., Lim, C. Y.,
1236   Rowe, J. C., Cox, J. L., Moss, J., Roscioli, J. R., Canagaratna, M. R., Worsnop, D. R.,
1237   Kroll, J. H. and Keutsch, F. N.: Mechanistic study of the formation of ring-retaining and
1238   ring-opening products from the oxidation of aromatic compounds under urban
1239   atmospheric conditions, Atmos. Chem. Phys., 19(23), 15117–15129, doi:10.5194/acp-19-
1240   15117-2019, 2019a.

1241   Zaytsev, A., Breitenlechner, M., Koss, A. R., Lim, C. Y., Rowe, J. C., Kroll, J. H. and
1242   Keutsch, F. N.: Using collision-induced dissociation to constrain sensitivity of ammonia
1243   chemical ionization mass spectrometry (NH4+ CIMS) to oxygenated volatile organic
1244   compounds, Atmos. Meas. Tech., 12(3), 1861–1870, doi:10.5194/AMT-12-1861-2019,
1245   2019b.

1246